

MOTION OF A FLEXIBLE HYDROFOIL NEAR A FREE SURFACE

By

JOE WILSON REECE

A DISSERTATION PRESENTED TO THE GRADUATE COUNCIL OF
THE UNIVERSITY OF FLORIDA
IN PARTIAL FULFILLMENT OF THE REQUIREMENTS FOR THE
DEGREE OF DOCTOR OF PHILOSOPHY

UNIVERSITY OF FLORIDA

December, 1963

ACKNOWLEDGMENTS

The author wishes to thank Dr. J. Siekmann, Chairman of his Supervisory Committee, for suggesting this problem and for his continued encouragement and counsel.

He is grateful to the other committee members, Dr. W. A. Nash, Head of the Advanced Mechanics Research Section, Dr. S. Y. Lu, Associate Professor in Engineering Mechanics, Dr. I. K. Ebciooglu, Assistant Professor in Engineering Mechanics, and Dr. C. B. Smith, Professor of Mathematics, for their encouragement and helpful criticism of the manuscript.

The author is also indebted to Dr. I. C. Statler, Head of the Applied Mechanics Department, Cornell Aeronautical Laboratory, for his timely suggestions and advice.

The author thanks Dr. Nash and Mr. B. M. Woodward, Manager of the University of Florida Computing Center, for providing financial assistance for the use of the IBM 709 digital computer.

To the Ford Foundation he expresses profound gratitude for supporting his graduate studies for the past twenty-seven months.

Finally, he is grateful to his wife, Nancy, for her support and understanding during a difficult time. She has been a "rock" in a sea of "free surface waves."

TABLE OF CONTENTS

	Page
ACKNOWLEDGMENTS	ii
LIST OF TABLES	v
LIST OF FIGURES	vi
LIST OF SYMBOLS	vii
ABSTRACT	x
INTRODUCTION	1
Chapter	
I. FORMULATION OF THE PROBLEM	5
1.1 The Motion of the Plate	
1.2 The Plate Model	
1.3 The Velocity Potential	
1.4 The Integral Equation	
II. SOLUTION OF THE INTEGRAL EQUATION	23
2.1 Form of the Solution	
2.2 Solution for the Infinite Set of Equations	
III. THE EFFECT OF THE FLOW ON THE PLATE	30
3.1 Pressure Distribution	
3.2 Lift and Moment	
3.3 Drag and Thrust	
IV. NUMERICAL EXAMPLE	46
4.1 Quadratically Varying Amplitude Function	
4.2 Solution of the Algebraic Equations	
4.3 The Resulting Thrust	

TABLE OF CONTENTS--Continued

	Page
V. SUMMARY AND CONCLUSIONS	58
Appendices	
A. THE FREE SURFACE POTENTIAL	63
B. COEFFICIENTS FOR THE INFINITE SET OF EQUATIONS	83
C. $\Delta p(\theta, t)$ FOR THE CASE IN WHICH $D \rightarrow \infty$	91
LIST OF REFERENCES	99
BIOGRAPHICAL SKETCH	102

LIST OF TABLES

Table	Page
1. Free Surface Flow Conditions	19
2. Real and Imaginary Parts of B_n and C_n	52
3. Thrust Coefficient	54
4. Thrust Coefficient	54
5. Variation of σ_j' , $j = 1, 2, 3, 4$, With kF^2	68
6. $\bar{G}(x, D; \xi)$ for $x \rightarrow \pm \infty$	74
7. $G(x, D; \xi)$ for $x \rightarrow \pm \infty$	79
8. Variation of S_j , $j = 1, 2, 3, 4$, With kF^2	81

LIST OF FIGURES

Figure	Page
1. The Flexible Plate	6
2. The Plate Model	6
3. Single Vortex Line	12
4. Vortex Sheet With Special Coordinates	12
5. Thrust Coefficient Versus Reduced Frequency	55
6. Thrust Coefficient Versus Reduced Frequency for Small Reduced Frequencies	57
7. Contours of Integration for the I_j' Integrals	69
8. Contour of Integration for I_1'	70
9. Contours of Integration for \bar{I}_j Integrals	76
10. Contour of Integration for \bar{I}_1	77

LIST OF SYMBOLS

A_n	Coefficient of the Fourier series giving the downwash on the plate
α_n	Coefficient of the series expansion for the pressure distribution $\Delta p(x, t)$
B_n	Coefficient of the Fourier series giving the displacement function of the plate
C_n	Coefficient of the Fourier series giving the slope of the plate
\tilde{C}_{mn}	Complex element of the coefficient matrix of the infinite set of algebraic equations
\tilde{C}'_{mn}	Real part of \tilde{C}_{mn}
\tilde{C}''_{mn}	Imaginary part of \tilde{C}_{mn}
C_T	Thrust coefficient
$C(k)$	Theodorsen function
c_o, c_1, c_2	Coefficients of the quadratic plate amplitude function
D	Depth of the plate compared to a semichord of 1
\tilde{D}	Drag
D_j	Constants related to the free surface radiation conditions ($j = 1, 2, 3, 4$)
d_n	Auxiliary coefficient used in the series for the pressure distribution
F	Froude number
$G(x, y; \xi)$	Auxiliary function related to the free surface potential

g	Acceleration due to gravity
$H_n^{(2)}(z)$	Hankel function of the second kind, n^{th} order, with argument z
$h(x, t)$	Displacement function for the oscillating plate
$J_n(s)$	Bessel function of n^{th} order with argument s
$K_n(z)$	Modified Bessel function of the second kind, n^{th} order, with argument z
k	Reduced frequency of the plate motion
L	Lift per unit span
M	Moment per unit span
p	Pressure
T	Thrust per unit span
\bar{T}	Time average value of the thrust
t	Time
U	Magnitude of the free stream velocity
u	Magnitude of the x -component of the perturbation velocity
v	Magnitude of the y -component of the perturbation velocity
$Y(x, t)$	Displacement in the y -direction of the plate
$Y_n(s)$	Neumann function of n^{th} order with argument s
α	Wave number of the plate motion
β	Auxiliary dissipative constant
Γ	Circulation
δ	Phase angle of the plate motion

$\gamma(x, t)$	Vortex strength distribution for the plate vortex sheet
$\xi(x, t)$	Vortex strength distribution for the wake vortex sheet
η	Coordinate of a vortex sheet in the y-direction
$\eta(x, t)$	Vertical displacement of the free surface relative to its mean position
Θ	Independent variable related to x by $x = -\cos \Theta$
λ	Wave length of the plate motion
μ	Dissipative constant
ξ	Coordinate of a vortex sheet in the x-direction
ρ	Mass density of the fluid
τ	Period of the plate motion
$\Phi(x, y, t)$	Total velocity potential function
$\Phi_i(x, y, t)$	Velocity potential due to the plate vortex sheet and its wake
$\Phi_z(x, y, t)$	Velocity potential due to the image system
$\Phi_i(x, y)$	Spatial part of $\Phi_i(x, y, t)$
ω	Circular frequency of the plate motion
Ω	External force potential
$i = \sqrt{-1}$	Imaginary unit
$\text{Re}\{f\}$	Denotes real part of f
$\text{Im}\{f\}$	Denotes imaginary part of f

Abstract of Dissertation Presented to the Graduate Council
in Partial Fulfillment of the Requirements for the
Degree of Doctor of Philosophy

MOTION OF A FLEXIBLE HYDROFOIL
NEAR A FREE SURFACE

By

Joe Wilson Reece

December, 1963

Chairman: Dr. Julius Siekmann

Major Department: Engineering Mechanics

This study consists of a theoretical investigation of the effect of free surface waves on the swimming of a thin, flexible, two-dimensional plate immersed in an ideal, incompressible fluid. The fluid is assumed to be infinitely deep, and the surface waves considered are those generated by the motion of the plate itself. It is assumed that the plate moves through the fluid at a constant rate, while executing lateral motion consisting of waves which travel from front to rear with increasing amplitude. The amplitude of the plate motion is made to depend, not only on time, but on the distance which the displacement wave has progressed from the leading edge of the plate. This type motion is used in order to simulate the swimming of a thin

fish near the surface of the water. Of particular interest is the thrust developed by the swimming action of the plate.

The mathematical theory used is based on velocity potential methods as employed in unsteady hydrofoil theory. In this theory the effect of the plate on the flow field is replaced by a continuous vortex sheet system of oscillating strength. An image system of vortices is postulated to lie out of the water just above the plate so that the net effect of the two systems causes no surface disturbance. This allows the potential of the surface waves to be investigated as a separate function through the free surface boundary conditions. A kinematic condition at the plate between the motion of the fluid and the motion of the plate leads to an integral equation for the vortex strength distribution. This distribution is governed by the integral equation in a spatial manner only as it has already been assumed oscillatory in the time variable due to the harmonic nature of the plate motion. The wake vortices shed at the trailing edge of the plate are accounted for in the analysis. They are assumed to lie in the plane of the plate and to be convected downstream with the free stream velocity.

The solution of the integral equation for the vortex strength distribution is effected by assuming a Glauert type of series result. This transforms the integral equation into an infinite system of inhomogeneous algebraic equations. These equations are solved by

truncating the set so as to ascertain as many of the unknowns as are needed for accuracy in the final solution. The resulting expression for the vortex strength distribution insures smooth attached flow at the plate trailing edge, thus satisfying the Kutta condition.

From this vortex strength distribution the hydrodynamic pressure acting on the plate is found through the use of the unsteady Euler equation. The lift and moment on the plate are calculated by integrating the pressure difference between the top and bottom sides of the plate along the chord of the plate. The thrust is obtained by integrating the product of the pressure difference and the local slope of the plate along the chord. It is demonstrated that for the case of swimming at infinite depth the results of this study and those obtained by other researchers are in agreement.

A numerical example is given for the case of plate motion with displacement waves whose amplitudes vary in a quadratic manner along the length of the plate. The time average value of the thrust over a period of the plate motion is computed for two different depths and several frequencies of plate motion. It is found that the influence of the free surface waves acts to decrease the available thrust. The decrease is more pronounced at high frequencies than at low frequencies.

INTRODUCTION

Of late, an increasing number of researchers have been inquiring into the matter of sea animal locomotion. The manner in which a fish swims has been viewed both as a biological and an engineering problem. Attention is called to the papers of Gawn [1, 2], Taylor [3, 4], Gray [5], Richardson [6], and Dickmann [7].

Two recent papers by Siekmann [8] and Wu [9] have established identical results for a fish model swimming horizontally with a constant velocity in an infinite, ideal, incompressible fluid. Both authors have used a flat plate of zero thickness, infinite span, and finite chord to approximate a thin fish. The plate experiences a traveling wave beginning at its leading edge and progressing toward its trailing edge with increasing amplitude. Wu attacks the problem using Prandtl's acceleration potential theory, while Siekmann approaches the problem through the airfoil flutter theory developed by Küssner and Schwarz [10], with particular reference to the paper by Schwarz [11].

Smith and Stone [12] have partially solved the same problem in an elliptic coordinate system, but they have failed to consider the wake effects. Their solution has recently been modified and extended to include the wake effects by Pao and Siekmann [13]. Results identical to those of Siekmann [8] and Wu [9] have been obtained.

In the present work the effect of a free surface on the swimming of the thin plate model is sought. As the plate approaches the vicinity of the surface, a disturbance arises on the surface which has an effect on the motion of the plate. Siekmann, Wu, and Pao have shown that a positive thrust is developed in case the frequency of the plate oscillation is sufficiently large. Some questions immediately arise when free surface effects are considered. Will the presence of the free surface provide an increase or a decrease in the thrust? Just how close to the surface does the plate have to be in order for the thrust to be influenced to any great extent?

As a starting point in the analysis, the particularly illuminating hydrofoil report by Crimi and Statler [14] is used. This report, concerning the motion of an oscillating rigid hydrofoil near the free surface of a liquid, is based on two papers by Tan [15, 16]. Tan has obtained the velocity potential of a point source or vortex line of fluctuating strength moving near the free surface of a liquid. In his second paper Tan investigates the behavior of the free surface and provides valuable information regarding the nature of the waves produced by a disturbing point source of fluctuating strength moving at a uniform rate near the surface. Crimi and Statler use essentially an integrated form of Tan's results for a moving point vortex of fluctuating strength. This idea is connected with airfoil flutter theory in that one way of approaching the problem is by replacing the thin plate by a vortex sheet of

fluctuating strength [17]. In such flutter theory and in the sea animal locomotion paper by Siekmann [8], an integral equation results for the strength of the vortex sheet. The formulation of the problem in an infinite flow results in a fairly simple integral equation of the form

$$\int_{-i}^i \frac{H(\xi)}{x - \xi} d\xi = G(x) + \lambda^* \int_1^\infty e^{-\sigma x'} \frac{1}{x - x'} dx' ,$$

where $H(\xi)$ is the sought for function related to the vortex distribution strength, and λ^* and σ are constants. This equation has been discussed by Söhngen [18], and the solution has been modified and used by Schwarz [11]. The presence of the free surface alters the form of the analogous integral equation and makes it much more complicated.

Crini and Statler have employed a method of solution giving results in approximate but extremely accurate form. In their solution none of the effects of the free surface are lost. A similar equation will result in the following analysis, and the same method will be used to solve it.

Other investigators have studied the effects of the free surface on an oscillating rigid hydrofoil, but several simplifying assumptions have been made in their work. Chu and Abramson [19] assumed an infinite Froude number allowing for no surface waves. Their solution is in the form of a chord-to-depth ratio expansion and therefore holds only for relatively high velocities and large submergence depths. Kaplan [20] has analyzed the same problem considering the primary effects

of a finite Froude number, but his model consists of a single vortex and a doublet and is not as precise as the model of Crimi and Statler.

It should be mentioned that the problem is formulated here and solved within the bounds of linear theory. The results obtained are perhaps as pertinent to the field of hydrofoil hydrodynamics as they are to sea animal locomotion.

CHAPTER I

FORMULATION OF THE PROBLEM

Consider the two-dimensional flow of an incompressible, inviscid fluid around a flexible solid plate of zero thickness. The flow is influenced by a free surface of the fluid. We allow that the plate spans from $x = -1$ to $x = +1$ and lies at a distance D beneath the mean free surface as shown in Figure 1.

An axes system is taken fixed in the plate with the x -axis in the direction of the flow. The flow, with constant velocity U , is allowed to stream over the undulating plate in the positive x -direction or in a left-to-right sense.

1.1 The Motion of the Plate

The deflection of the solid deformable plate is taken as

$$y = h(x, t) , \quad -1 \leq x \leq +1 , \quad (1.1)$$

and it is assumed that these deflections are small with respect to the chord of the plate, i. e.,

$$|y| \ll 1 , \quad \left| \frac{\partial y}{\partial x} \right| \ll 1 , \quad \left| \frac{\partial y}{\partial t} \right| \ll 1 . \quad (1.2)$$

If we assume that the motion of the plate consists of a traveling wave of small amplitude, we may write

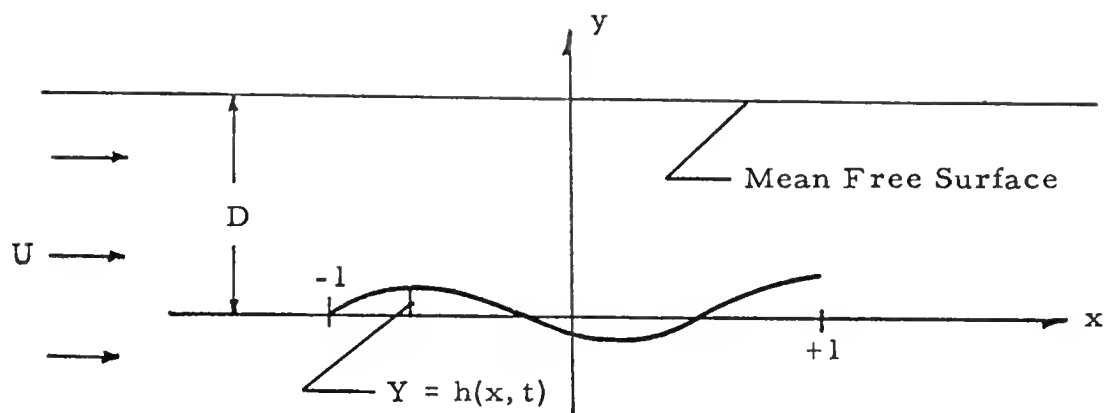


Figure 1. The Flexible Plate

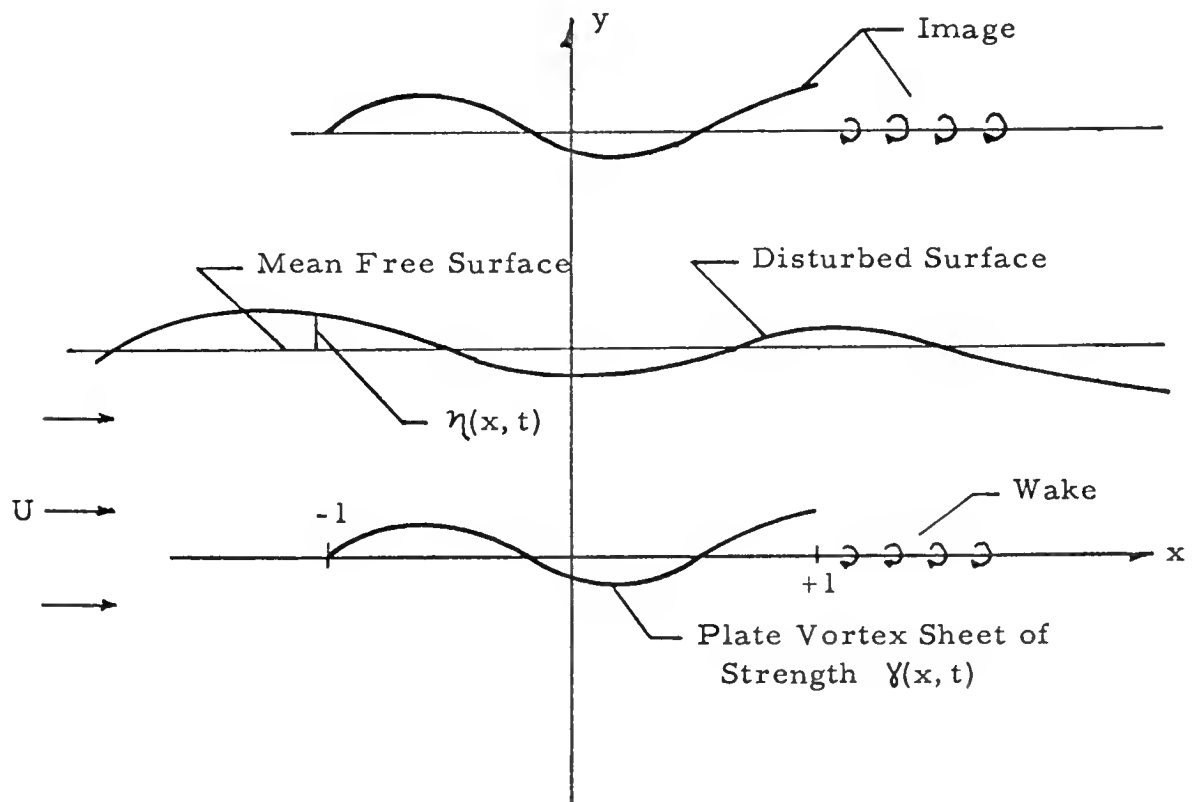


Figure 2. The Plate Model

$$Y = h(x, t) = f(x) \cos(\alpha x - \omega t + \delta), -1 \leq x \leq 1 \quad (1.3)$$

in which $f(x)$ is the amplitude function of the wave, α is the wave number, ω is the circular frequency, and δ is the phase angle. Upon insertion of the wave length λ

$$\lambda = \frac{2\pi}{\alpha}, \quad (1.4)$$

the period τ

$$\tau = \frac{2\pi}{\omega}, \quad (1.5)$$

and the propagation velocity V

$$V = \frac{\omega}{\alpha}, \quad (1.6)$$

the plate displacement can be written as

$$Y = h(x, t) = f(x) \cos \frac{2\pi}{\lambda} \left(x - Vt + \frac{\lambda \delta}{2\pi} \right). \quad (1.7)$$

Such motion can also be described generally by

$$Y = H(x) e^{i\omega t} \quad (1.8)$$

if the real part is used for a physical interpretation. It should be noted that $H(x)$ may be complex.

1.2 The Plate Model

The deformable solid plate is replaced by a vortex sheet of oscillating strength. As the circulation is time varying, vorticity must be shed into the wake in order to satisfy Kelvin's circulation theorem [21]. These shed vortices are carried downstream with the free stream velocity U . Hence, the model of the plate and its total effect on the flow is represented by the plate vortex sheet and its trailing

vortex wake. It is also assumed that the shed vortex trail lies in the plane $y = 0$. This is not precisely the case, but the assumption greatly simplifies the analysis.

In order to satisfy the free surface conditions, an image system is located 2D units above the plane $y = 0$. This image system consists of a vortex sheet along with its trailing shed vortices identical to the plate system located in the plane $y = 0$ (see Fig. 2). Thus, the combined effect of the plate system of vortices and its image is to make the free surface appear as undisturbed. As the surface will obviously be disturbed, a means must be found which will allow the determination of the effect of the disturbed surface on the flow.

1.3 The Velocity Potential

An obvious method of attack is seen in the use of potential theory in the case of nonaccelerated flow. The potential due to the vortex sheet of oscillating strength over the plate as well as that of its image may be written down. The same holds true for the vortices in the wake and their images. Then, a potential function for the effect of the free surface may be postulated and a partial differential equation found for its determination. Thus, a total perturbation velocity potential $\Phi(x, y, t)$ is postulated which takes into account the effect of the plate system of vortices and its wake, the image system of vortices and its wake in addition to the effect of the disturbed free surface.

We assume that the velocity vector \bar{q} of the flow is given by

$$\bar{q} = \{U + u, v\} , \quad (1.9)$$

where u and v are the x and y perturbation components of the velocity

$$u = \frac{\partial \Phi}{\partial x} , \quad v = \frac{\partial \Phi}{\partial y} . \quad (1.10)$$

This means that we have assumed irrotational flow. Upon substituting (1.10) into the continuity equation

$$\operatorname{div} \bar{q} = 0 \quad (1.11)$$

for incompressible flow, we see that the velocity potential, Φ , must satisfy the Laplace equation

$$\nabla^2 \Phi = 0. \quad (1.12)$$

Hence, Φ is a harmonic function of the space variables in the field of the flow.

The potential, Φ , must also satisfy certain boundary conditions. If the free surface disturbance given by

$$y = \eta(x, t)$$

is to be a stream line, then

$$\frac{d\eta}{dt} = \frac{\partial \eta}{\partial t} + \frac{\partial \eta}{\partial x} \frac{dx}{dt} = \frac{\partial \Phi}{\partial y} , \quad y = D. \quad (1.13)$$

If the total velocity vector is taken in the form given by (1.9), equation (1.13) becomes

$$\frac{\partial \Phi}{\partial y} = \frac{\partial \eta}{\partial t} + (U + u) \frac{\partial \eta}{\partial x} , \quad y = D , \quad (1.14)$$

which, in the bounds of linear theory, is altered to

$$\frac{\partial \Phi}{\partial y} = \frac{\partial \eta}{\partial t} + U \frac{\partial \eta}{\partial x} , \quad y = 0. \quad (1.15)$$

The unsteady Bernoulli equation

$$\frac{1}{2} |\bar{q}|^2 + \frac{\partial \Phi}{\partial t} + \Omega + \frac{p}{\rho} = w(t) , \quad y = 0 , \quad (1.16)$$

must also be satisfied at the free surface. In equation (1.16), p is the pressure at the free surface, ρ is the density of the fluid, $w(t)$ is an arbitrary function of time which can be specified by the flow conditions at infinity, and Ω is the external force potential given by

$$\Omega = gn.$$

If the velocity vector \bar{q} and the force potential Ω are inserted into equation (1.16), and if the pressure is required to equal that at infinity, i.e., a constant, the equation becomes

$$uU + \frac{1}{2}(u^2 + v^2) + \frac{\partial \Phi}{\partial t} = -gn , \quad y = 0 , \quad (1.17)$$

where g is the acceleration due to gravity. Again, due to the linear theory, this boundary condition may be simplified to read

$$\frac{\partial \Phi}{\partial t} + U \frac{\partial \Phi}{\partial x} = -gn , \quad y = 0 . \quad (1.18)$$

For the third boundary condition the fact that the plate is a solid impenetrable body is used. The corresponding kinematic condition

$$\frac{\partial y}{\partial t} = -(U + u) \frac{\partial y}{\partial x} + v , \quad y = 0 , \quad (1.19)$$

must be met. This relation is also linearized to

$$v_p = \frac{\partial \Phi}{\partial y} = \frac{\partial y}{\partial t} + U \frac{\partial y}{\partial x} , \quad y = 0 , \quad (1.20)$$

where v_p is the fluid velocity in the vertical direction of a particle adjacent to the plate.

It should also be noted that the Kutta condition should be satisfied at the trailing edge of the plate.

Having set forth the fundamental equations governing the behavior of the velocity potential, we are now in a position to proceed to the development of the various potential functions.

Consider the single vortex line of fluctuating strength located at the origin as in Figure 3. The velocity potential of this vortex line as given in polar coordinates is

$$\hat{\phi}(r, \theta, t) = \frac{\Gamma(t) \theta}{2\pi} , \quad (1.21)$$

or in rectangular coordinates

$$\hat{\phi}(x, y, t) = -\frac{\Gamma(t)}{2\pi} \tan^{-1} \frac{y}{x} , \quad (1.22)$$

where $\Gamma(t)$ is the total time varying circulation.

For a vortex sheet of strength $\gamma(\xi, t)$ located at a $\xi \ll b$, $y = \eta$ as in Figure 4, the contribution to the infinitesimal element of the velocity potential $d\Phi^*$ at the point (x, y) due to the infinitesimal element of the sheet $d\xi$ is given by

$$d\Phi^* = -\frac{\gamma(\xi, t)}{2\pi} \tan^{-1} \frac{y-\eta}{x-\xi} d\xi , \quad (1.23)$$

and the potential due to the whole sheet is

$$\Phi^* = -\frac{1}{2\pi} \int_{\xi=a}^{\xi=b} \gamma(\xi, t) \tan^{-1} \frac{y-\eta}{x-\xi} d\xi . \quad (1.24)$$

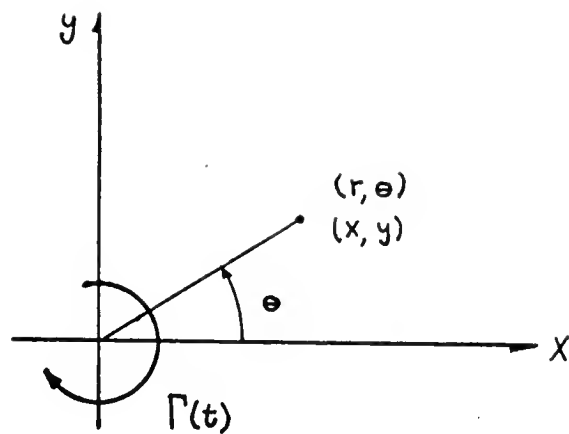


Figure 3. Single Vortex Line

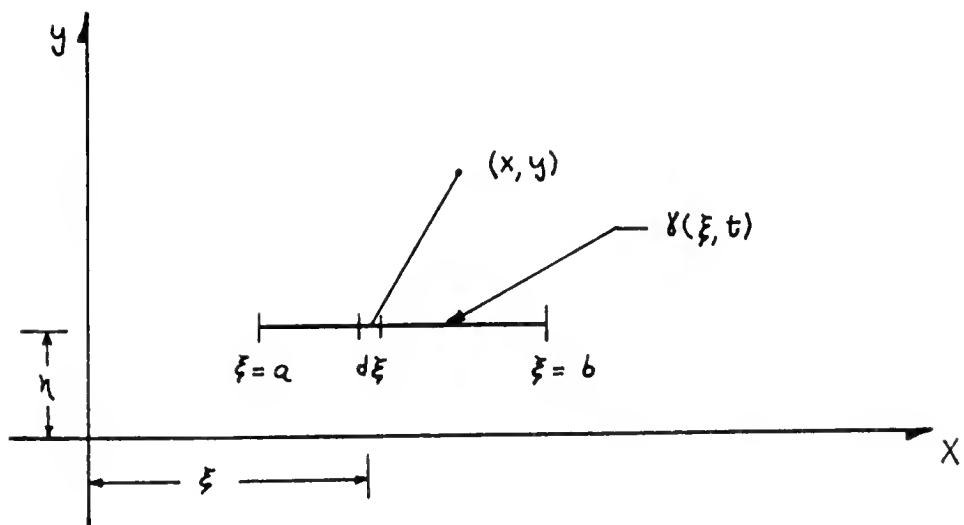


Figure 4. Vortex Sheet With Special Coordinates

The circulation around the vortex sheet is given by

$$\Gamma(t) = \int_a^b \gamma(x, t) dx \quad (1.25)$$

and is taken positive in a clockwise direction.

Since the circulation is time varying, it is obvious that vorticity must be shed into the wake to satisfy Kelvin's theorem. Denoting the strength of these vortices shed at the trailing edge of the plate by $\varepsilon(x, t)$ as in Figure 2, and observing that they are carried away by the free stream velocity U , we write

$$\varepsilon(x, t) = \varepsilon(x - Ut_o, t - t_o) , \quad t_o = \frac{x-1}{U} , \quad (1.26)$$

or

$$\varepsilon(x, t) = \varepsilon(1, t - \frac{x-1}{U}) , \quad x > 1 . \quad (1.27)$$

The change in circulation around the plate in time dt is

$$\frac{d\Gamma}{dt} dt \quad (1.28)$$

and is of equal magnitude and opposite in sign to the vortex

$$\varepsilon(1, t) dx , \quad dx = U dt , \quad (1.29)$$

shed at the trailing edge. Thus,

$$\begin{aligned} \varepsilon(1, t) dx &= U \varepsilon(1, t) dt \\ &= \left[- \int_{-1}^1 \frac{\partial}{\partial t} \gamma(\xi, t) d\xi \right] dt . \end{aligned} \quad (1.30)$$

Using (1.27), the vortex strength in the wake becomes

$$\varepsilon(x, t) = - \frac{1}{U} \int_{-1}^1 \frac{\partial}{\partial t} \gamma(\xi, t - \frac{x-1}{U}) d\xi , \quad x > 1 . \quad (1.31)$$

Now it seems reasonable to assume that

$$\gamma(x, t) = \gamma(x) e^{i\omega t} \quad (1.32)$$

since the motion of the plate is harmonic. Hence, it follows from (1.31) that

$$\begin{aligned} \epsilon(x, t) &= -\frac{i\omega}{U} \int_{-1}^1 e^{i\omega(t - \frac{x-1}{U})} \gamma(\xi) d\xi \\ &= -\frac{i\omega}{U} e^{i\omega t} \int_{-1}^1 e^{-\frac{i\omega}{U}(x-1)} \gamma(\xi) d\xi \\ &= -\frac{i\omega}{U} e^{i\omega t} e^{-i\omega(\frac{x-1}{U})} \int_{-1}^1 \gamma(\xi) d\xi. \end{aligned} \quad (1.33)$$

If we recall (1.25) defining the total circulation around the plate and use the standard form for the reduced frequency

$$\kappa = \frac{\omega}{U}, \quad (1.34)$$

the wake vortex strength becomes

$$\epsilon(x, t) = -i\kappa e^{i\omega t} \bar{\Gamma} e^{i\kappa(x-1)}, \quad (1.35)$$

where

$$\bar{\Gamma} = \int_{-1}^1 \gamma(x) dx \quad (1.36)$$

so that

$$\bar{\Gamma} e^{i\omega t} = \Gamma. \quad (1.37)$$

Upon applying equation (1.24) for the plate vortex sheet and again for its wake and adding, there results the potential due to the entire vortex sheet which is denoted by

$$\Phi_1 = -\frac{1}{2\pi} e^{i\omega t} \left\{ \int_{-1}^1 y(\xi) \tan^{-1} \frac{y}{x-\xi} d\xi + i\kappa \bar{\Gamma} \int_1^\infty e^{-i\kappa(\xi-1)} \tan^{-1} \frac{y-zD}{x-\xi} d\xi \right\}. \quad (1.38)$$

For the image system we write correspondingly

$$\Phi_2 = -\frac{1}{2\pi} e^{i\omega t} \left\{ \int_{-1}^1 y(\xi) \tan^{-1} \frac{y-zD}{x-\xi} d\xi + i\kappa \bar{\Gamma} \int_1^\infty e^{-i\kappa(\xi-1)} \tan^{-1} \frac{y-zD}{x-\xi} d\xi \right\}. \quad (1.39)$$

The two potential functions Φ_1 and Φ_2 are clearly harmonic.

It is not unreasonable to expect the third potential function Φ_3 , due to the disturbed surface, to be harmonic also. Hence, we write

$$\Phi(x, y, t) = \operatorname{Re} \left[\{ \Phi_1 + \Phi_2 + \Phi_3 \} e^{i\omega t} \right], \quad (1.40)$$

where

$$\Phi_j(x, y, t) = \varphi_j(x, y) e^{i\omega t}, \quad j = 1, 2, 3,$$

and $\varphi_j(x, y)$ is to be taken as the spatial part of each potential function $\Phi_j(x, y, t)$. To investigate the nature of φ_3 , we combine the boundary conditions (1.15) and (1.18) by eliminating $\eta(x, t)$ to get

$$\frac{\partial^2 \Phi}{\partial t^2} + 2U \frac{\partial^2 \Phi}{\partial t \partial x} + U^2 \frac{\partial^2 \Phi}{\partial x^2} = -g \frac{\partial \Phi}{\partial y}, \quad y = 0. \quad (1.41)$$

If equations (1.38) and (1.39) are rewritten using

$$\Phi_1 = \varphi_1(x, y) e^{i\omega t}, \quad \Phi_2 = \varphi_2(x, y) e^{i\omega t},$$

and substituted into equation (1.41), it is not difficult to obtain a partial differential equation for Φ_3 in the form

$$\begin{aligned} \frac{\partial^2 \Phi_3}{\partial x^2} + z i k \frac{\partial \Phi_3}{\partial x} + \frac{1}{F^2} \frac{\partial \Phi_3}{\partial y} - k^2 \Phi_3 &= \\ \frac{1}{\pi F^2} \int_{-1}^1 \frac{\gamma(\xi)(x-\xi)}{(x-\xi)^2 + D^2} d\xi \\ - \frac{i k \bar{\Gamma}}{\pi F^2} \int_1^\infty \frac{e^{-i k(\xi-1)} (x-\xi)}{(x-\xi)^2 + D^2} d\xi \quad , \end{aligned} \quad (1.42)$$

where the Froude number F is given by

$$F = \frac{v}{\sqrt{g}} . \quad (1.43)$$

Tan [15] has solved a partial differential equation similar to (1.42) in the case of a single vortex of oscillating strength. Hence, according to Crimi and Statler [14], the solution to (1.42) can be obtained by taking an integral form of Tan's results as

$$\begin{aligned} \Phi_3(x, y) &= \frac{i}{2\pi F^2} \int_{-1}^1 \gamma(\xi) G(\xi; x, y) d\xi + \\ &+ \frac{k \bar{\Gamma}}{2\pi F^2} \int_1^\infty e^{-i k(\xi-1)} G(\xi; x, y) d\xi , \end{aligned} \quad (1.44a)$$

where

$$\begin{aligned}
 G(\xi; x, y) = & \int_0^\infty e^{s(y-2D)} \left[\frac{e^{is(x-\xi)}}{(s-s_1)(s-s_2)} - \frac{e^{-is(x-\xi)}}{(s-s_3)(s-s_4)} \right] ds + \\
 & + D_1 e^{s_1[y-2D+i(x-\xi)]} + D_2 e^{s_2[y-2D+i(x-\xi)]} + \\
 & + D_3 e^{s_3[y-2D-i(x-\xi)]} + D_4 e^{s_4[y-2D-i(x-\xi)]}, \quad (1.44b)
 \end{aligned}$$

and

$$\left. \begin{aligned}
 (s-s_1)(s-s_2) &= s^2 - \left(\frac{1}{F^2} - 2K \right) s + K^2 \\
 (s-s_3)(s-s_4) &= s^2 - \left(\frac{1}{F^2} + 2K \right) s + K^2
 \end{aligned} \right\}. \quad (1.44c)$$

We refer to Appendix A for a more detailed explanation.

The terms of (1.44) involving the double integration give a particular solution to (1.43), and the remaining terms containing the D_1 , D_2 , D_3 , and D_4 are the complementary solution. Obviously, the solution is incomplete in this form since we do not yet know the D_j . The constants D_j will have to be determined by the free surface flow conditions at infinity.

A detailed analysis of the free surface flow conditions is provided in Tan's paper [16] for the case of a single source of fluctuating strength, and a similar analysis is outlined in the paper of Crimi and Statler [14] for a vortex sheet of fluctuating strength. The method employed was first used by Rayleigh [22] and constitutes the introduction of a small fictitious dissipative force - $\mu \operatorname{grad} \Phi$, $\mu > 0$. The results are then examined as μ tends to zero in the limit.

Crimi and Statler have shown that the constants D_j may be assigned to provide the correct free surface flow conditions depending upon the following combination of the Froude number and the reduced frequency: kF^2 .

The values of the D_j as so determined are reproduced in tabular form as a convenience in Table 1. Appendix A offers an analysis in some detail leading to these constants.

In examining the table we note that for $kF^2 > 0$, S_3 and S_4 will be real and positive so that at least two harmonic wave trains always exist on the surface. Their wave lengths are $2\pi/S_3$ and $2\pi/S_4$. They propagate downstream from the plate and cannot exist physically upstream of the plate.

For $kF^2 > 1/4$, the roots S_1 and S_2 are complex conjugates and therefore produce damped waves which do not influence the flow at great distances from the plate. In case $kF^2 < 1/4$, S_1 and S_2 are real and positive. The group velocity of the wave arising from S_1 is less than U , requiring that this wave trail the plate. The S_2 wave has a group velocity greater than U and will lead the plate. Thus, there are two harmonic waves propagating upstream for $0 < kF^2 < 1/4$, one leading and one trailing the plate.

In the special case $kF^2 = 0$ (steady motion), the only roots present are S_1 and S_3 . The solutions combine to give a single standing wave of wave length $2\pi U^2/g$ downstream of the plate. Let us refer to

TABLE 1
FREE SURFACE FLOW CONDITIONS

kF^2	S_1, S_2	S_3, S_4	FLOW CONDITIONS				D_1	D_2	D_3	D_4
			Downstream	$x \rightarrow +\infty$	Upstream	$x \rightarrow -\infty$				
0	$\frac{1}{F^2}, 0$	$\frac{1}{F^2}, 0$	Single harmonic wave Wave length: $\frac{2\pi U^2}{g}$		Undisturbed		$\frac{\pi i}{S_1}$	0	$\frac{\pi i}{S_3}$	0
$0 < kF^2 < \frac{1}{4}$	Real and Positive	Real and Positive	Three harmonic waves: Wave lengths: $\frac{2\pi}{S_1}, \frac{2\pi}{S_3}, \frac{2\pi}{S_4}$		Single harmonic wave Wave length: $\frac{2\pi}{S_2}$		$\frac{\pi i}{S_1 - S_2}$	$\frac{\pi i}{S_1 - S_2}$	$\frac{\pi i}{S_3 - S_4}$	$\frac{-\pi i}{S_3 - S_4}$
$\frac{1}{4} < kF^2$	Complex	Real and Positive	Two harmonic waves Wave lengths: $\frac{2\pi}{S_3}, \frac{2\pi}{S_4}$		Undisturbed		0	0	$\frac{\pi i}{S_3 - S_4}$	$\frac{\pi i}{S_3 - S_4}$

Note: S_1, S_2 - upstream-propagating waves; S_3, S_4 -- downstream-propagating waves.

Source: Crimi and Statler [14].

the paper by Isay [23] for a solution to the problem of a flat plate in steady motion moving near the free surface.

When $kF^2 = 1/4$, the integral associated with $G(\xi; x, y)$ does not exist. The roots S_1 and S_2 do exist, however, but the group velocities of the associated waves are the same, creating a resonance condition. Thus, for a given flow velocity U and, hence, for a given Froude number F , there exists a critical frequency, k_{critical} , for which $(k_{\text{critical}})F^2 = 1/4$, and for which no solution exists within the framework of the present formulation.

1.4 The Integral Equation

The last step in the actual formulation of the problem requires that the boundary condition on the plate be used. From the last section we see that with the use of equations (1.38), (1.39), and (1.44) the total potential given by

$$\Phi(x, y, t) = \operatorname{Re} \{ \Phi_1 + \Phi_2 + \Phi_3 \} e^{i\omega t}$$

is known except for the vortex strength distribution $\gamma(\xi)$. If the boundary condition (1.20) relating the velocity of a fluid particle near the plate to the motion of the plate is used, there results an integral equation for the determination of the vortex strength distribution. If we keep in mind the type of motion which is to be imposed on the plate, namely that given by equation (1.8), then the boundary condition (1.20) becomes

$$\frac{\partial \bar{\Phi}}{\partial y} = -U [H'(x) + ikH(x)] e^{i\omega t}, \quad y=0, \quad (1.45)$$

where

$$H'(x) = \frac{dH}{dx}.$$

Upon substituting the determined value of $\bar{\Phi}$ in (1.45), there results

the integral equation

$$\begin{aligned} \frac{1}{2\pi} \int_{-1}^1 \frac{y(\xi)}{x-\xi} d\xi &= -\frac{1}{2\pi} \int_{-1}^1 y(\xi) \left[\frac{x-\xi}{(x-\xi)^2 + 4D^2} - \frac{i}{F^2} \left. \frac{\partial G(\xi; x, y)}{\partial y} \right|_{y=0} \right] d\xi + \\ &+ \frac{ik\bar{\Pi}}{2\pi} \int_1^\infty e^{-ik(\xi-1)} \left[\frac{1}{x-\xi} + \frac{x-\xi}{(x-\xi)^2 + 4D^2} - \frac{i}{F^2} \left. \frac{\partial G(\xi; x, y)}{\partial y} \right|_{y=0} \right] d\xi + \\ &+ U [H'(x) + ikH(x)]; \quad y=0, \quad -1 \leq x \leq 1, \quad (1.46) \end{aligned}$$

where the Cauchy principal value is to be taken for the integral on the left-hand side, and the quantity $\left. \frac{\partial G}{\partial y} \right|_{y=0}$ is found to be from (1.44b):

$$\begin{aligned} \left. \frac{\partial G(\xi; x, y)}{\partial y} \right|_{y=0} &= \int_0^\infty s e^{-2Ds} \left[\frac{e^{is(x-\xi)}}{(s-s_1)(s-s_2)} - \frac{e^{-is(x-\xi)}}{(s-s_3)(s-s_4)} \right] ds + \\ &+ s_1 D_1 e^{s_1 [-2D+i(x-\xi)]} + s_2 D_2 e^{s_2 [-2D+i(x-\xi)]} \\ &+ s_3 D_3 e^{s_3 [-2D-i(x-\xi)]} + s_4 D_4 e^{s_4 [-2D-i(x-\xi)]}. \end{aligned}$$

In addition to the requirement that $y(\xi)$ satisfy the integral equation (1.46), $y(\xi)$ must produce a velocity field which allows a finite velocity at the trailing edge of the plate.

If D is allowed to approach infinity in the integral equation, another integral equation results, governing the value of $y(\xi)$ for the

case of infinite flow about the oscillating plate. In this case the equation becomes

$$\frac{1}{2\pi} \oint_{-1}^1 \frac{\gamma(\xi)}{x - \xi} d\xi = \frac{i\kappa \bar{r}}{2\pi} \int_1^\infty \frac{e^{-ik(\xi-1)}}{x - \xi} d\xi + G^*(x)$$

which is seen to be equivalent to the equation investigated by Söhngen [18] and applied by Siekmann [8] to the study of sea animal locomotion.

With the derivation of the integral equation (1.46), the formulation of the problem is complete.

CHAPTER II

SOLUTION OF THE INTEGRAL EQUATION

As mentioned in the Introduction and demonstrated at the end of Chapter I, the formulation of the problem of an oscillating hydrofoil or thin plate in infinite flow ($D \rightarrow \infty$) leads to a well-known integral equation. The presence of a free surface obviously has complicated the integral equation considerably, as evidenced by equation (1.46). An approximate method of attack seems to be the most expedient way of solving this equation. It is possible to make the final results as accurate as desired through the use of high-speed computing techniques.

2.1 Form of the Solution

Crimi and Statler [14] have been successful in solving an integral equation much like (1.46). Equation (1.46) differs from the one solved by Crimi and Statler in that an infinite number of terms enter due to the plate boundary condition.

We first assume that the vortex strength distribution $\gamma(\theta)$ is given by the Glauert trigonometric series

$$\gamma(\theta) = 2U \left[a_0 \cot \frac{\theta}{2} + \sum_{n=1}^{\infty} a_n \sin n\theta \right] , \quad (2.1)$$

where $x = -\cos \theta$, $-1 \leq x \leq +1$, $0 \leq \theta \leq 2\pi$, and the α_n may be complex.

It is easy to find the total circulation around the plate with this form of the vortex strength distribution. From (1.36) and (2.1), $\bar{\Gamma}$ is calculated as

$$\begin{aligned}
 \bar{\Gamma} &= \int_{-1}^1 \gamma(x) dx = \int_0^\pi \gamma(\theta) \sin \theta d\theta \\
 &= 2U \int_0^\pi \left[\alpha_0 \cot \frac{\theta}{2} + \sum_{n=1}^{\infty} \alpha_n \sin n\theta \right] \sin \theta d\theta \\
 &= 2\pi U \left(\alpha_0 + \frac{\alpha_1}{2} \right) . \tag{2.2}
 \end{aligned}$$

Substituting (2.1) into the left side of the integral equation (1.46), there results after the integration

$$\frac{1}{2\pi} \int_{-1}^1 \frac{\gamma(\xi)}{x - \xi} d\xi = U \left[\alpha_0 - \sum_{n=1}^{\infty} \alpha_n \cos n\theta \right] . \tag{2.3}$$

Now, if the right-hand side of (1.46) can be expressed as a Fourier cosine series, like coefficients of $\cos n\theta$ can be equated to obtain an infinite set of inhomogeneous algebraic equations involving an infinite number of unknown α_n . The expansion of the right-hand side of (1.46) involves much manipulative work. Fortunately, the results of Crimi and Statler can be used, as the only differing terms are incorporated in the inhomogeneous terms of the infinite set of equations:

$$a_m = \sum_{n=0}^{\infty} C_{mn} a_n + r_m ; \quad m = 0, 1, 2, \dots \quad (2.4)$$

Crими and Statler have considered the motion of a hydrofoil with two degrees of freedom, pitching and plunging, whereas, the inhomogeneous terms of (2.4) reduce to only two, r_0 and r_1 . The oscillating plate dealt with in this work has an infinite number of degrees of freedom. Thus, as might be expected, an infinite number of inhomogeneous terms are involved.

The technique used in expanding the integral expressions in the right-hand side of (1.46) deserves mention. Consider the integral

$$I_1 = \frac{i \kappa \bar{\Gamma}}{2\pi} \int_1^{\infty} \frac{e^{-i\kappa(\xi-1)} (x-\xi)}{(x-\xi)^2 + 4D^2} d\xi , \quad (2.5)$$

where $x = -\cos \theta$. Now in transform theory, the Laplace transform of a function $\hat{F}(s)$ is

$$\hat{f}(q) = \mathcal{L}\{\hat{F}(s)\} = \int_0^{\infty} e^{-qs} \hat{F}(s) ds ,$$

and in particular

$$\frac{a}{q^2 + a^2} = \mathcal{L}\{\sin as\} . \quad (2.6)$$

In the fraction of the integrand in (2.5)

$$\frac{-(\cos \theta + \xi)}{(2D)^2 + (\cos \theta + \xi)^2}$$

let $a = (\cos \theta) + \xi$ and $q = 2D$ when applying (2.6). Thus,

$$-\frac{\cos \theta + \xi}{(2D)^2 + (\xi + \cos \theta)^2} = \frac{1}{2i} \int_0^\infty e^{-2Ds} \left[e^{-is(\xi + \cos \theta)} - e^{+is(\xi + \cos \theta)} \right] ds. \quad (2.7)$$

Letting

$$-\frac{\cos \theta + \xi}{(2D)^2 + (\xi + \cos \theta)^2} = \frac{b_0}{2} + \sum_{n=1}^{\infty} b_n \cos n\theta, \quad (2.8)$$

and employing (2.7), the b_n Fourier coefficient is given by

$$\begin{aligned} b_n &= \frac{1}{\pi i} \int_0^\infty e^{-2Ds} \left[e^{-is\xi} \int_0^\pi e^{-is\cos \theta} \cos n\theta d\theta \right. \\ &\quad \left. - e^{-is\xi} \int_0^\pi e^{is\cos \theta} \cos n\theta d\theta \right] ds \\ &= i^{n+1} \int_0^\infty e^{-2Ds} J_n(s) \left[e^{+is\xi} - (-1)^n e^{-is\xi} \right] ds. \quad (2.9) \end{aligned}$$

In the last step the integral formula

$$\begin{aligned} J_n(s) &= \frac{i^{-3n}}{\pi} \int_0^\pi e^{-is\cos \theta} \cos n\theta d\theta \\ &= \frac{i^{-n}}{\pi} \int_0^\pi e^{is\cos \theta} \cos n\theta d\theta \end{aligned}$$

for the Bessel function J_n of the first kind and order n has been used.

Inserting the total circulation $\bar{\Gamma}$ from (2.2), the integral I_1 can now be written as

$$I_1 = ikU \left(a_0 + \frac{a_1}{2} \right) \int_1^\infty e^{-ik(\xi-1)} \left[\frac{b_0}{2} + \sum_{n=1}^\infty b_n \cos n\theta \right] d\xi . \quad (2.10)$$

Finally, if b_n from (2.9) is placed in (2.10), and the ξ is integrated out, I_1 can be written as

$$I_1 = ikU \left(a_0 + \frac{a_1}{2} \right) \left[\frac{\bar{b}_0}{2} + \sum_{n=1}^\infty \bar{b}_n \cos n\theta \right] , \quad (2.11)$$

where

$$\bar{b}_n = i^n \int_0^\infty e^{-2\theta s} J_n(s) \left[\frac{e^{is}}{k-s} - (-1)^n \frac{e^{-is}}{k+s} \right] ds .$$

Other of the integrals are less difficult to expand. Consider the integral

$$I_2 = \frac{ik\bar{b}}{2\pi} \int_1^\infty \frac{e^{-ik(\xi-1)}}{x-\xi} d\xi , \quad (2.12)$$

where $x = -\cos \theta$. Assume that

$$I_2 = \frac{c_0}{2} + \sum_{n=1}^\infty c_n \cos n\theta . \quad (2.13)$$

Then,

$$c_n = -\frac{2ikU}{\pi} \left(a_0 + \frac{a_1}{2} \right) \int_0^\pi \int_1^\infty \frac{e^{-ik(\xi-1)} \cos n\theta}{\xi + \cos \theta} d\xi d\theta .$$

Interchanging the order of integration and integrating with respect to ξ , we obtain

$$c_n = -2kU \left(a_0 + \frac{a_1}{2} \right) \int_1^\infty \frac{e^{-ik(\xi-1)} (\xi - \sqrt{\xi^2 - 1})^n}{\sqrt{\xi^2 - 1}} d\xi . \quad (2.14)$$

When expansions for all the integrals on the right-hand side of (1.46) are found, the like coefficients of $\cos n\theta$ are equated, giving expressions for the \tilde{C}_{mn} terms of (2.4). These are listed by Crimi and Statler and are reproduced in Appendix B for convenience.

Return now to the inhomogeneous terms of the infinite set of equations. If the "downwash"

$$-U [H'(x) + ik H(x)] e^{i\omega t}$$

is assumed equal to the Fourier expansion

$$-U e^{i\omega t} \left[\frac{A_0}{2} + \sum_{n=1}^{\infty} A_n \cos n\theta \right] , \quad (2.15)$$

then it is easy to see that the inhomogeneous terms of (2.4) are

$$r_0 = \frac{A_0}{2}$$

$$r_m = -A_m , \quad m = 1, 2, 3, \dots \quad (2.16)$$

Note that the A_n are assumed known, as are the \tilde{C}_{mn} . The integrals involved in the \tilde{C}_{mn} cannot generally be expressed in closed form, but they may be calculated for various flow conditions by utilizing a high-speed computer.

We are now in a position to consider the infinite set of equations

$$a_m = \sum_{n=0}^{\infty} \tilde{C}_{mn} a_n + r_m , \quad (2.17)$$

seeking a solution for the a_n 's.

2.2 Solution for the Infinite Set of Equations

Some of the fundamental theorems dealing with a system of equations like (2.4) are presented in the book by Kantorovich and Krylov [24]. In certain cases it is possible to show that a solution exists and is unique. Such is not the case here, but we expect that a solution exists due to the behavior of the \tilde{C}_{mn} and the r_m for increasing m and n . The \tilde{C}_{mn} decrease rapidly when either m or n increases or when both m and n increase. In the particular example to be considered in Chapter IV, it will be shown that the r_m decrease also with increasing m .

Assuming that a solution does exist, the procedure leading to an approximate solution is as follows [24]. We first find the solution to a reduced finite system of equations

$$a_m = \sum_{n=0}^N \tilde{C}_{mn} a_n + r_m ; \quad m = 0, 1, 2, \dots, N , \quad (2.18)$$

and then repeat the process for $N + 1$. This, of course, introduces an additional unknown, a_{N+1} , but at the same time limiting values for a_0 , a_1 , a_2 , \dots , $a_{M < N}$ become apparent. It develops that only a finite number of the a_m will be needed to define the lift and moment on the plate, but the thrust involves an infinite sum of the a_m which converge very rapidly. Also, it becomes apparent that approximately $N + 4$ complex equations of the set (2.4) need be solved to ascertain N of the a_m to a reasonable degree of accuracy.

CHAPTER III

THE EFFECT OF THE FLOW ON THE PLATE

In this chapter the forces and moments acting on the oscillating plate are discussed. Due to the unsteadiness of the motion, a pressure difference results between the top and bottom of the plate. This pressure difference is not constant, but varies with time and the x -coordinate along the plate in the chordwise direction. The first task is to derive an expression for this pressure difference distribution along the plate.

3.1 Pressure Distribution

If the pressures at the top and bottom sides of the plate are denoted by p^+ and p^- respectively, the pressure difference is given by

$$\Delta p = p^- - p^+ , \quad (3.1)$$

where it is assumed that the Δp will be positive in a sense implied by equation (3.1). This is in conformity with the negative direction for the downwash assumed in deriving the integral equation (1.46) governing the vortex distribution along the plate.

Considering the velocity vector \bar{q} to be given as in (1.9), the unsteady Euler equation

$$\frac{\partial u}{\partial t} + (U + u) \frac{\partial u}{\partial x} + V \frac{\partial u}{\partial y} = -\frac{1}{\rho} \frac{\partial p}{\partial x} \quad (3.2)$$

may be linearized to read

$$\frac{\partial u}{\partial t} + U \frac{\partial u}{\partial x} = -\frac{1}{\rho} \frac{\partial p}{\partial x} . \quad (3.3)$$

Writing the last equation for the top side of the plate,

$$\frac{\partial u^+}{\partial t} + U \frac{\partial u^+}{\partial x} = -\frac{1}{\rho} \frac{\partial p^+}{\partial x} ,$$

and for the bottom side,

$$\frac{\partial u^-}{\partial t} + U \frac{\partial u^-}{\partial x} = -\frac{1}{\rho} \frac{\partial p^-}{\partial x} ,$$

and subtracting one from the other, we obtain

$$\frac{\partial (u^+ - u^-)}{\partial t} + U \frac{\partial (u^+ - u^-)}{\partial x} = \frac{1}{\rho} \frac{\partial \Delta p}{\partial x} . \quad (3.4)$$

Now $u^+ - u^-$ is exactly the strength, $\gamma(x, t)$, of an element of the vortex sheet which we have allowed to replace the plate. Hence, we can rewrite (3.4) as

$$\frac{\partial \gamma}{\partial t} + U \frac{\partial \gamma}{\partial x} = \frac{1}{\rho} \frac{\partial \Delta p}{\partial x} . \quad (3.5)$$

If the total vortex sheet $\gamma(x, t)$ is divided into bound vortices $\gamma^*(x, t)$ and free vortices $\varepsilon^*(x, t)$, as in the paper by Schwarz [11], so that

$$\gamma(x, t) = \gamma^*(x, t) + \varepsilon^*(x, t) , \quad -1 \leq x \leq 1 , \quad (3.6)$$

we may substitute this expression in the second term of (3.5) to get

$$\frac{\partial \gamma}{\partial t} + U \left(\frac{\partial \gamma^*}{\partial x} + \frac{\partial \varepsilon^*}{\partial x} \right) = \frac{1}{\rho} \frac{\partial \Delta p}{\partial x} . \quad (3.7)$$

Now, according to the Kutta-Joukowski law

$$\Delta p = \rho U \gamma^*. \quad (3.8)$$

Using this in (3.7), the equation becomes

$$\frac{\partial \gamma}{\partial t} + U \frac{\partial \varepsilon^*}{\partial x} = 0, \quad (3.9)$$

giving a relation between the total vortex sheet and the free vortices.

Integrating (3.9) for $\varepsilon^*(x, t)$,

$$\varepsilon^*(x, t) = -\frac{1}{U} \int_{-1}^x \frac{\partial \gamma(\xi, t)}{\partial t} d\xi \quad ; -1 \leq x \leq 1,$$

and inserting the result in (3.6), we obtain

$$\gamma^*(x, t) = \gamma(x, t) + \frac{1}{U} \int_{-1}^x \frac{\partial \gamma(\xi, t)}{\partial t} d\xi. \quad (3.10)$$

In Chapter II we assumed the vortex distribution $\gamma(x, t)$ to be given by the Glauert trigonometric series

$$\gamma(\theta, t) = 2U \left[a_0 \cot \frac{\theta}{2} + \sum_{n=1}^{\infty} a_n \sin n\theta \right] e^{i\omega t},$$

where $x = -\cos \theta$. Placing this expression in (3.10), there results

$$\begin{aligned} \gamma^*(\theta, t) &= \gamma(\theta, t) + 2i\omega e^{i\omega t} \left[\int_0^\theta a_0 \cot \frac{\varphi}{2} \sin \varphi d\varphi \right. \\ &\quad \left. + \int_0^\theta \sum_{n=1}^{\infty} a_n \sin n\varphi \sin \varphi d\varphi \right]. \\ &= \gamma(\theta, t) + 2i\omega e^{i\omega t} [I_1^* + I_2^*]. \end{aligned} \quad (3.11)$$

Carrying out the indicated integrations for I_1^* and I_2^* , we obtain

$$I_1^* = \alpha_0 (\theta + \sin \theta)$$

$$I_2^* = \sum_{n=1}^{\infty} \frac{\alpha_n}{2} \left[\frac{\sin(n-1)\theta}{n-1} - \frac{\sin(n+1)\theta}{n+1} \right],$$

giving for $\gamma^*(\theta, t)$

$$\gamma^*(\theta, t) = \gamma(\theta, t) + 2i\omega e^{i\omega t} \left\{ \alpha_0 (\theta + \sin \theta) + \sum_{n=1}^{\infty} \frac{\alpha_n}{2} \left[\frac{\sin(n-1)\theta}{n-1} - \frac{\sin(n+1)\theta}{n+1} \right] \right\}. \quad (3.12)$$

Finally, after a little manipulation, the pressure distribution $\Delta p(\theta, t)$ is obtained from (3.8) as

$$\Delta p(\theta, t) = 2\rho U^2 e^{i\omega t} \left\{ \alpha_0 \cot \frac{\theta}{2} + \left(\alpha_1 + i\kappa [3\alpha_0 + \alpha_1 + \frac{\alpha_2}{2}] \right) \sin \theta + \sum_{n=2}^{\infty} \left[\alpha_n + \frac{i\kappa}{2n} \left(\alpha_{n+1} - \alpha_{n-1} + 2(2\alpha_0 + \alpha_1)(-1)^{n+1} \right) \right] \sin n\theta \right\}. \quad (3.13)$$

It is pertinent to note that this expression reduces to that derived by Siekmann [8] for the case $D \rightarrow \infty$. (See Appendix C.)

3.2 Lift and Moment

With the expression for $\Delta p(\theta, t)$ given by (3.13) at hand, it is easy to compute the lift and moment acting on the plate. In computing the lift, the pressure should be allowed to act in a normal direction to the surface of the plate (which is constantly changing), but as small

deformations have been assumed, it is within keeping with the linear theory to assume that the pressure acts normal to the x-axis. Hence, the lift is given by

$$L = \int_{-1}^1 \Delta p(x, t) dx , \quad (3.14)$$

and the moment by

$$M = \int_{-1}^1 x \Delta p(x, t) dx , \quad (3.15)$$

where the moment is considered positive in a clockwise sense and is calculated with respect to the origin, $x = 0, y = 0$. Inserting Δp from (3.13) and changing the variable according to $x = -\cos \theta$, we may

write

$$L = \rho U \int_0^\pi \gamma^*(\theta, t) \sin \theta d\theta , \quad (3.16)$$

and

$$M = -\rho U \int_0^\pi \gamma^*(\theta, t) \sin \theta \cos \theta d\theta . \quad (3.17)$$

It remains now only to use the expression derived for $\gamma^*(\theta, t)$ from Section 3.1 and carry out the indicated integration with respect to θ . The resulting expressions for the lift and moment are respectively

$$L = 2\pi \rho U^2 e^{i\omega t} \left[\left(a_0 + \frac{a_1}{2} \right) + \frac{i\kappa}{2} \left(3a_0 + a_1 + \frac{a_2}{2} \right) \right] , \quad (3.18)$$

and

$$M = \rho \pi U^2 e^{i\omega t} \left[\left(a_0 + \frac{a_2}{2} \right) + \frac{i\kappa}{2} \left(a_0 + \frac{3a_1}{4} - \frac{a_3}{4} \right) \right]. \quad (3.19)$$

In calculating the moment, the pressure difference Δp has again been assumed to act normal to the x-axis, and the leading edge suction force [8] has been neglected.

3.3 Drag and Thrust

The drag or thrust experienced by the undulating plate will result due to the x-component of the hydrodynamic pressure difference Δp . It can readily be seen that the horizontal hydrodynamic force on a plate element of projection dx on the x-axis is given by

$$\operatorname{Re} \{ \Delta p \} \operatorname{Re} \left\{ \frac{\partial Y}{\partial x} \right\} dx. \quad (3.20)$$

The real parts, denoted by $\operatorname{Re} \{ \cdot \}$, are taken because nonlinear terms enter the product which involve mixed expressions in \dot{U} . Thus, over the whole plate the hydrodynamic force in the positive x-direction is given by

$$\tilde{D} = \tilde{D}_p + \tilde{D}_s = \int_{-1}^1 \operatorname{Re} \{ \Delta p \} \operatorname{Re} \left\{ \frac{\partial Y}{\partial x} \right\} dx + \tilde{D}_s, \quad (3.21)$$

where \tilde{D}_s is the leading edge suction force.

The plate displacement $Y(x, t)$ given by equation (1.8) is an even function of Θ , where $x = -\cos \Theta$ due to the fact that the plate is very thin, thus allowing a point on the bottom side of the plate to be represented by the same coordinates as the adjacent point on the top side of

the plate. Hence, $Y(x, t)$ can be expanded in a Fourier cosine series of θ as

$$Y(x, t) = H(x) e^{i\omega t} = \left[\frac{B_0}{2} + \sum_{n=1}^{\infty} B_n \cos n\theta \right] e^{i\omega t}, \quad (3.22)$$

where

$$B_n = \frac{2}{\pi} \int_0^{\pi} H(x) \cos n\theta d\theta = \frac{2}{\pi} \int_0^{\pi} \tilde{H}(\theta) \cos n\theta d\theta. \quad (3.23)$$

The slope, $\frac{\partial Y}{\partial x}$, can also be expressed as a Fourier cosine series since the plate is infinitesimally thin. First, note that from

$$\tilde{Y}(\theta, t) = \tilde{H}(\theta) e^{i\omega t}, \quad (3.24)$$

there results

$$\frac{\partial \tilde{Y}(\theta, t)}{\partial x} = \frac{\partial \tilde{Y}}{\partial \theta} \frac{\partial \theta}{\partial x},$$

and as $x = -\cos \theta$, we have

$$\frac{\partial \tilde{Y}}{\partial x} = \frac{1}{\sin \theta} \frac{\partial \tilde{Y}}{\partial \theta} = \frac{1}{\sin \theta} \dot{\tilde{H}} e^{i\omega t}, \quad (3.25)$$

where

$$\frac{d \tilde{H}}{d \theta} = \dot{\tilde{H}}.$$

Now we can write

$$\frac{\partial \tilde{Y}(\theta, t)}{\partial x} = \left[\frac{C_0}{2} + \sum_{n=1}^{\infty} C_n \cos n\theta \right] e^{i\omega t}, \quad (3.26)$$

where

$$C_n = \frac{2}{\pi} \int_0^{\pi} \dot{\tilde{H}}(\theta) \frac{\cos n\theta}{\sin \theta} d\theta. \quad (3.27)$$

There is obviously a relation between the C's and the B's. This follows from (3.22) with

$$H'(x) = -2 \sum_{n=1}^{\infty} n B_n \frac{\sin n\theta}{\sin \theta} . \quad (3.28)$$

Upon comparing (3.28) and (3.26), we get

$$C_{n-1} - C_{n+1} = -2n B_n ; \quad n = 1, 2, \dots , \quad (3.29)$$

or

$$C_{2n} = -2 \sum_{m=n}^{\infty} (2m+1) B_{2m+1} ; \quad n = 0, 1, 2, \dots \quad (3.30)$$

$$C_{2n+1} = -2 \sum_{m=n}^{\infty} (2m+2) B_{2m+2} ; \quad n = 0, 1, 2, \dots \quad (3.31)$$

In Section 2.1 it was assumed that the portion of the downwash given by

$$[H'(x) + i k H(x)] e^{i \omega t} \quad (3.32)$$

was expressible as a Fourier series like

$$\left[\frac{A_0}{z} + \sum A_n \cos n\theta \right] e^{i \omega t} . \quad (3.33)$$

This assumption, together with equations (3.22) and (3.26), allows the conclusion that the following relation must exist between the A's, B's, and C's:

$$A_n = C_n + i k B_n . \quad (3.34)$$

As only the real parts of Δp and $\frac{\partial Y}{\partial x}$ are used in computing the horizontal force \tilde{D} , the notation is best altered to denote this fact.

Following Siekmann [8], we define

$$A_n e^{i\omega t} = (A'_n + i A''_n) e^{i\omega t} = \bar{A}'_n + i \bar{A}''_n , \quad (3.35a)$$

$$B_n e^{i\omega t} = (B'_n + i B''_n) e^{i\omega t} = \bar{B}'_n + i \bar{B}''_n , \quad (3.35b)$$

$$C_n e^{i\omega t} = (C'_n + i C''_n) e^{i\omega t} = \bar{C}'_n + i \bar{C}''_n , \quad (3.35c)$$

where

$$\bar{A}'_n = A'_n \cos \omega t - A''_n \sin \omega t , \quad (3.36a)$$

$$\bar{A}''_n = A''_n \cos \omega t + A'_n \sin \omega t , \quad (3.36b)$$

and so forth. Then, for the real part of $\frac{\partial Y}{\partial X}$, we have

$$\operatorname{Re} \left\{ \frac{\partial Y}{\partial X} \right\} = \frac{\bar{C}_0'}{2} + \sum_{n=1}^{\infty} \bar{C}'_n \cos n\theta . \quad (3.37)$$

The notation will be simplified somewhat if the pressure distribution $\Delta p(\theta, t)$ is written from (3.13) as

$$\Delta p(\theta, t) = 2\rho U^2 e^{i\omega t} \left[a_0 \cot \frac{\theta}{2} + d_1 \sin \theta + \sum_{n=2}^{\infty} d_n \sin n\theta \right] , \quad (3.38)$$

where

$$d_1 = a_1 + ik [3a_0 + a_1 + \frac{a_2}{2}] , \quad (3.39)$$

$$d_n = a_n + \frac{ik}{2n} \left[a_{n+1} - a_{n-1} + 2(z a_0 + a_1) (-1)^{n+1} \right] , n \geq 2 . \quad (3.40)$$

Analogous to equations (3.35) and (3.36), we define

$$a_n e^{i\omega t} = (a'_n + i a''_n) e^{i\omega t} = \bar{a}'_n + i \bar{a}''_n , \quad (3.41a)$$

$$d_n e^{i\omega t} = (d'_n + i d''_n) e^{i\omega t} = \bar{d}'_n + i \bar{d}''_n , \quad (3.41b)$$

where

$$\bar{a}_n' = a_n' \cos \omega t - a_n'' \sin \omega t, \quad (3.42a)$$

$$\bar{a}_n'' = a_n'' \cos \omega t + a_n' \sin \omega t. \quad (3.42b)$$

Then the real part of $\Delta p(\theta, t)$ is given by

$$\operatorname{Re}\{\Delta p\} = 2\rho U^2 \left[\bar{a}_0' \cot \frac{\theta}{2} + \bar{d}_1' \sin \theta + \sum_{n=2}^{\infty} \bar{d}_n' \sin n\theta \right]. \quad (3.43)$$

The portion of the horizontal force \tilde{D} denoted by \tilde{D}_p follows from integrating

$$\begin{aligned} \tilde{D}_p = 2\rho U^2 \int_0^{\pi} & \left\{ \bar{a}_0' \cot \frac{\theta}{2} + \bar{d}_1' \sin \theta + \right. \\ & \left. + \sum_{n=2}^{\infty} \bar{d}_n' \sin n\theta \right\} \cdot \left\{ \frac{\bar{C}_0'}{2} + \sum_{m=1}^{\infty} \bar{C}_m' \cos m\theta \right\} \sin \theta \, d\theta. \end{aligned} \quad (3.44)$$

Multiplying $\sin \theta$ with the first braced quantity and employing the trigonometric identity

$$\sin n\theta \sin \theta = \frac{1}{2} [\cos(n-1)\theta - \cos(n+1)\theta],$$

we may write (3.44) as

$$\begin{aligned} \tilde{D}_p = 2\rho U^2 \int_0^{\pi} & \left\{ \bar{a}_0' \cot \frac{\theta}{2} \sin \theta + \bar{d}_1' \sin^2 \theta + \right. \\ & + \frac{1}{2} \sum_{n=2}^{\infty} \bar{d}_n' [\cos(n-1)\theta - \cos(n+1)\theta] \left. \right\} \cdot \left\{ \frac{\bar{C}_0'}{2} + \right. \\ & \left. + \sum_{m=1}^{\infty} \bar{C}_m' \cos m\theta \right\} \, d\theta. \end{aligned} \quad (3.45)$$

Using the idea of the Cauchy product in the integrand of (3.45) and interchanging the order of integration and summation, \tilde{D}_p may be written as

$$\begin{aligned}
 \tilde{D}_p = & 2 \rho V^z \left\{ \frac{\tilde{C}_0'}{2} \int_0^{\pi} \left(\tilde{a}_0' \cot \frac{\theta}{2} \sin \theta + \tilde{d}_1' \sin^2 \theta \right) d\theta + \right. \\
 & + \frac{\tilde{C}_0'}{4} \sum_{n=2}^{\infty} \tilde{d}_n' \int_0^{\pi} [\cos(n-1)\theta - \cos(n+1)\theta] d\theta + \\
 & + \tilde{a}_0' \sum_{m=1}^{\infty} \tilde{C}_m' \int_0^{\pi} \cot \frac{\theta}{2} \sin \theta \cos m\theta d\theta + \\
 & + \tilde{d}_1' \sum_{m=1}^{\infty} \tilde{C}_m' \int_0^{\pi} \sin^2 \theta \cos m\theta d\theta + \\
 & \left. + \frac{1}{2} \sum_{n=2}^{\infty} \sum_{m=1}^{\infty} \tilde{d}_n' \tilde{C}_m' \int_0^{\pi} [\cos(n-1)\theta - \cos(n+1)\theta] \cos m\theta d\theta \right\}. \tag{3.46}
 \end{aligned}$$

The definite integrals in equation (3.46) are evaluated as

$$\int_0^{\pi} \cot \frac{\theta}{2} \sin \theta d\theta = \pi \tag{3.47a}$$

$$\int_0^{\pi} \sin^2 \theta d\theta = \frac{\pi}{2} \tag{3.47b}$$

$$\int_0^{\pi} \cos(n-1)\theta d\theta = 0 \quad n \geq 2 \tag{3.47c}$$

$$\int_0^\pi \cos(n+1)\theta d\theta = 0 \quad n \geq 2 \quad (3.47d)$$

$$\int_0^\pi \cot\frac{\theta}{2} \sin\theta \cos m\theta d\theta = \begin{cases} \frac{\pi}{2} & m = 1 \\ 0 & m > 1 \end{cases} \quad (3.47e)$$

$$\int_0^\pi \sin^2\theta \cos m\theta d\theta = \begin{cases} 0 & m = 1 \\ -\frac{\pi}{4} & m = 2 \\ 0 & m > 2 \end{cases} \quad (3.47f)$$

$$\int_0^\pi \cos(n-1)\theta \cos m\theta d\theta = \frac{\pi}{2} \quad m = n-1 \quad (3.47g)$$

$$\int_0^\pi \cos(n+1)\theta \cos m\theta d\theta = \frac{\pi}{2} \quad m = n+1 \quad (3.47h)$$

Using these definite integral values in equation (3.46), we write

\tilde{D}_p as

$$\begin{aligned} \tilde{D}_p = \pi \rho U^2 & \left\{ \bar{C}_0' \left(\bar{\alpha}_0' + \frac{\bar{d}_1'}{2} \right) + \bar{\alpha}_0' \bar{C}_1' - \frac{\bar{d}_1' \bar{C}_2'}{2} + \right. \\ & \left. + \frac{1}{2} \sum_{n=2}^{\infty} \bar{d}_n' \left(\bar{C}_{n-1}' - \bar{C}_{n+1}' \right) \right\} . \end{aligned} \quad (3.48)$$

Recalling equation (3.29), the last term in (3.48) may be

written as

$$- \sum_{n=2}^{\infty} n \bar{d}_n' \bar{B}_n' . \quad (3.49)$$

From equations (3.39) and (3.40), keeping in mind the notation indicated by equations (3.41) and (3.42), we may write

$$\bar{d}'_1 = \bar{\alpha}'_1 - \kappa (3\bar{\alpha}''_0 + \bar{\alpha}''_1 + \frac{\bar{\alpha}''_z}{z}) , \quad (3.50)$$

and

$$\bar{d}'_n = \bar{\alpha}'_n - \frac{\kappa}{zn} \left[\bar{\alpha}''_{n+1} - \bar{\alpha}''_{n-1} + 2(z\bar{\alpha}''_0 + \bar{\alpha}''_1)(-1)^{n+1} \right] . \quad (3.51)$$

Using (3.50) and (3.51) in equation (3.48), the horizontal force \tilde{D}_p is written as

$$\begin{aligned} \tilde{D}_p = & \rho \pi U^2 \left\{ \bar{\alpha}'_0 (\bar{C}'_0 + \bar{C}'_1) + \right. \\ & + \frac{1}{2} (\bar{C}'_0 - \bar{C}'_z) \left[\bar{\alpha}'_1 - \kappa (3\bar{\alpha}''_0 + \bar{\alpha}''_1 + \bar{\alpha}''_z/z) \right] - \\ & - \sum_{n=2}^{\infty} n \bar{\alpha}'_n \bar{B}'_n + \frac{\kappa}{2} \sum_{n=2}^{\infty} \bar{B}'_n (\bar{\alpha}''_{n+1} - \bar{\alpha}''_{n-1}) + \\ & \left. + \kappa (z\bar{\alpha}''_0 + \bar{\alpha}''_1) \sum_{n=2}^{\infty} (-1)^{n+1} \bar{B}'_n \right\} . \end{aligned} \quad (3.52)$$

The suction force due to the singularity at the leading edge of the plate is discussed by Siekmann [8]. The contribution of this singularity to the horizontal force acts in the negative x-direction, hence the terminology "suction force." Its magnitude is

$$\tilde{D}_s = 2\pi \rho U^2 \bar{\alpha}'_0^2 . \quad (3.53)$$

Therefore, the total horizontal force acting in the positive x-direction, or the drag, is given by

$$\tilde{D} = \tilde{D}_p - \tilde{D}_s = \tilde{D}_p - 2\pi \rho U^2 \bar{a}_o'^2. \quad (3.54)$$

The thrust is clearly the negative of this quantity and is written from equations (3.52) and (3.53) as

$$\begin{aligned} T = \pi \rho U^2 & \left\{ 2\bar{a}_o'^2 - \bar{a}_o' (\bar{C}_o' + \bar{C}_i') + \right. \\ & + \frac{1}{2} (\bar{C}_2' - \bar{C}_o') \left[\bar{a}_i' - \kappa (3\bar{a}_o'' + \bar{a}_i'' + \frac{\bar{a}_2''}{2}) \right] + \\ & + \sum_{n=2}^{\infty} n \bar{a}_n' \bar{B}_n' - \frac{\kappa}{2} \sum_{n=2}^{\infty} \bar{B}_n' (\bar{a}_{n+1}'' - \bar{a}_{n-1}'') - \\ & \left. - \kappa (2\bar{a}_o'' + \bar{a}_i'') \sum_{n=2}^{\infty} (-1)^{n+1} \bar{B}_n' \right\}. \quad (3.55) \end{aligned}$$

Instead of this expression for the thrust, it is more meaningful to calculate its time average value over a period $\tilde{\tau}$. The time average value of a function $\psi(t)$ is defined as

$$\bar{\psi}^* = \frac{1}{\tilde{\tau}} \int_0^{\tilde{\tau}} \psi(t) dt. \quad (3.56)$$

Because of the relations (3.36), need for the following will arise:

$$\begin{aligned} \bar{\psi}_1^* &= \frac{1}{\tilde{\tau}} \int_0^{\tilde{\tau}} \cos^2 \omega t dt = \frac{1}{2} \\ \bar{\psi}_2^* &= \frac{1}{\tilde{\tau}} \int_0^{\tilde{\tau}} \sin^2 \omega t dt = \frac{1}{2} \\ \bar{\psi}_3^* &= \frac{1}{\tilde{\tau}} \int_0^{\tilde{\tau}} \sin \omega t \cos \omega t dt = 0 \quad \left. \right\} \end{aligned} \quad (3.57)$$

where $\mathcal{T} = 2\pi/\omega$. Keeping equations (3.36) and (3.57) in mind, the various products in the time average value of the thrust,

$$\bar{T}^* = \frac{1}{\mathcal{T}} \int_0^{\mathcal{T}} T(t) dt, \quad (3.58)$$

are

$$\frac{1}{\mathcal{T}} \int_0^{\mathcal{T}} \bar{C}_n' \bar{a}_m' dt = \frac{1}{2} (C_n' a_m' + C_n'' a_m'') \quad (3.59a)$$

$$\frac{1}{\mathcal{T}} \int_0^{\mathcal{T}} \bar{C}_n' \bar{a}_m'' dt = \frac{1}{2} (C_n' a_m'' - C_n'' a_m') \quad (3.59b)$$

$$\frac{1}{\mathcal{T}} \int_0^{\mathcal{T}} \sum_{n=2}^{\infty} n \bar{a}_n' \bar{B}_n' dt = \frac{1}{2} \sum_{n=2}^{\infty} n (a_n' B_n' + a_n'' B_n'') \quad (3.59c)$$

$$\frac{1}{\mathcal{T}} \int_0^{\mathcal{T}} \sum_{n=2}^{\infty} \bar{B}_n' (\bar{a}_{n+1}'' - \bar{a}_{n-1}'') dt =$$

$$\frac{1}{2} \sum_{n=2}^{\infty} B_n' (a_{n+1}'' - a_{n-1}'') - B_n'' (a_{n+1}' - a_{n-1}')$$

$$(3.59d)$$

$$\frac{1}{\mathcal{T}} \int_0^{\mathcal{T}} \bar{a}_m'' \sum_{n=2}^{\infty} (-1)^{n+1} \bar{B}_n' dt = \frac{1}{2} \sum_{n=2}^{\infty} (-1)^{n+1} (a_m'' B_n' - a_m' B_n''). \quad (3.59e)$$

Inserting these representative values in (3.55), the time average value of the thrust is given by

$$\begin{aligned}
 \overset{*}{T} = & \frac{\pi \rho U^2}{2} \left\{ \alpha'_0 (2\alpha'_0 - C'_0 - C'_1) + \alpha''_0 (2\alpha''_0 - C''_0 - C''_1) + \right. \\
 & + \frac{1}{2} (C'_2 - C'_0) \left[\alpha'_1 - K(3\alpha''_0 + \alpha''_1 + \frac{\alpha''_2}{2}) \right] + \\
 & + \frac{1}{2} (C''_2 - C''_0) \left[\alpha''_1 + K(3\alpha'_0 + \alpha'_1 + \frac{\alpha'_2}{2}) \right] + \\
 & + \sum_{n=2}^{\infty} n (\alpha'_n B'_n + \alpha''_n B''_n) - \\
 & - \frac{K}{2} \sum_{n=2}^{\infty} B'_n (\alpha''_{n+1} - \alpha''_{n-1}) - B''_n (\alpha'_{n+1} - \alpha'_{n-1}) - \\
 & \left. - K(2\alpha''_0 + \alpha''_1) \sum_{n=2}^{\infty} (-1)^{n+1} B'_n + K(2\alpha'_0 + \alpha'_1) \sum_{n=2}^{\infty} (-1)^{n+1} B''_n \right\}. \quad (3.60)
 \end{aligned}$$

Finally, a thrust coefficient C_T is defined as

$$C_T = \frac{\overset{*}{T}}{\pi \rho U^2} . \quad (3.61)$$

Substituting (3.60) in (3.61) gives the thrust coefficient in terms of the α 's (the solution of the infinite set of algebraic equations), the B 's (the Fourier coefficients of the deflection function's expansion), the C 's (the Fourier coefficients of the slope function's expansion), and the flow parameters U , ρ , and K .

CHAPTER IV

NUMERICAL EXAMPLE

In accordance with the idea of representing the motion of a thin flat fish with a two-dimensional thin waving plate, we consider an appropriate displacement function and calculate numerical results for the thrust coefficient in this chapter. It is desired to compare these results with those of Siekmann [8] for the case of swimming at infinite depth so as to effectively isolate the influence of the free surface on the thrust.

4.1 Quadratically Varying Amplitude Function

Photographic analyses of swimming fish indicate that the motion of the fish is perhaps best represented by a quadratically varying amplitude function like

$$y = h(x, t) = (c_0 + c_1 x + c_2 x^2) \cos(\alpha x - \omega t), \quad (4.1)$$

where the c 's are constants. The notation here is in conformity with equation (1.3). The phase angle δ has been taken as zero.

In the last chapter the thrust coefficient was shown to be a function of the Fourier coefficients, B_n and C_n , and the Q_n which are the solution to the truncated set of equations represented by equation (2.18).

Also, the inhomogeneous terms of this set of equations are related to the B_n and C_n coefficients through equations (2.16) and (3.34). Thus, we first calculate the B_n and C_n coefficients associated with an amplitude function like that given by equation (4.1). Corresponding to the notation

$$Y(x, t) = H(x) e^{i\omega t},$$

$H(x)$ is given by

$$H(x) = (c_0 + c_1 x + c_2 x^2) e^{-i\alpha x}. \quad (4.2)$$

With $x = -\cos \theta$, we have

$$\tilde{H}(\theta) = (c_0 - c_1 \cos \theta + c_2 \cos^2 \theta) e^{i\alpha \cos \theta}. \quad (4.3)$$

Therefore, from equation (3.23) we have

$$B_n = \frac{2}{\pi} \int_0^\pi (c_0 - c_1 \cos \theta + c_2 \cos^2 \theta) e^{i\alpha \cos \theta} \cos n\theta d\theta. \quad (4.4)$$

Using the integral formula [25]

$$J_n(\alpha) = \frac{i^{-n}}{\pi} \int_0^\pi e^{i\alpha \cos \theta} \cos n\theta d\theta, \quad (4.5)$$

there results

$$B_n = i^n \left\{ 2c_0 J_n(\alpha) + c_2 \left[J_n(\alpha) - \frac{1}{2} (J_{n+2}(\alpha) + J_{n-2}(\alpha)) \right] - i c_1 \left[J_{n+1}(\alpha) - J_{n-1}(\alpha) \right] \right\}, \quad (4.6)$$

where the identity

$$\cos \theta \cos n\theta = \frac{1}{2} [\cos(n+1)\theta + \cos(n-1)\theta]$$

has been used. A similar calculation starting with equation (3.27)

yields the following for the C_n :

$$C_n = i^n \left\{ 2c_1 J_n(\alpha) - \pi c_1 [J_{n+1}(\alpha) - J_{n-1}(\alpha)] - \right. \\ - i \left(2\pi \left[c_0 + \frac{c_2}{2} \right] J_n(\alpha) + 2c_2 [J_{n+1}(\alpha) - \right. \\ \left. \left. - J_{n-1}(\alpha)] - \frac{c_2 \pi}{2} [J_{n+2}(\alpha) + J_{n-2}(\alpha)] \right) \right\} \quad (4.7)$$

To solve the truncated set of algebraic equations for the A_n , we will separate the set of N complex equations into two sets of N real equations each. This operation is necessary because the coefficients and the inhomogeneous terms are themselves complex. We have already indicated the complex nature of the B_n and C_n coefficients through the primed notation of the last chapter. Adhering to this notation, the real part of the B_n is

$$B'_n = (-1)^{\frac{n}{2}+2} \left\{ 2c_0 J_n(\alpha) + c_2 \left[J_n(\alpha) - \frac{1}{2} (J_{n+2}(\alpha) + J_{n-2}(\alpha)) \right] \right\} \quad (4.8) \quad n = 0, 2, 4, \dots$$

$$B'_n = (-1)^{\frac{n+3}{2}} \left\{ c_1 \left[J_{n+1}(\alpha) - J_{n-1}(\alpha) \right] \right\} \quad (4.9) \quad n = 1, 3, 5, \dots$$

The imaginary part of the B_n is

$$B''_n = (-1)^{\frac{n}{2}+1} \left\{ c_1 \left[J_{n+1}(\alpha) - J_{n-1}(\alpha) \right] \right\} \quad (4.10) \quad n = 0, 2, 4, \dots$$

$$B''_n = (-1)^{\frac{n+3}{2}} \left\{ 2c_0 J_n(\alpha) + c_2 \left[J_n(\alpha) - \frac{1}{2} (J_{n+2}(\alpha) + J_{n-2}(\alpha)) \right] \right\} \quad (4.11) \quad n = 1, 3, 5, \dots$$

For purposes of calculation it is desirable to eliminate the possibility of a negative order for any of the Bessel functions. Using the following

recursion formula [26]

$$J_{n+1}(\alpha) + J_{n-1}(\alpha) = \frac{2n}{\pi} J_n(\alpha)$$

as many times as necessary, there results

$$B'_n = (-1)^{\frac{n}{2}+2} 2 \left\{ (c_0 + c_2) J_n(\alpha) - \frac{c_2}{\pi} \left[\frac{n(n-1)}{\pi} J_n(\alpha) + J_{n+1}(\alpha) \right] \right\} \quad n=0,2,4,\dots \quad (4.12)$$

$$B'_n = (-1)^{\frac{n+3}{2}} 2 c_1 \left\{ J_{n+1}(\alpha) - \frac{n}{\pi} J_n(\alpha) \right\} \quad n=1,3,5,\dots \quad (4.13)$$

for the real part of B_n , and for the imaginary part

$$B''_n = (-1)^{\frac{n}{2}+1} 2 c_1 \left\{ J_{n+1}(\alpha) - \frac{n}{\pi} J_n(\alpha) \right\} \quad n=0,2,4,\dots \quad (4.14)$$

$$B''_n = (-1)^{\frac{n+3}{2}} 2 \left\{ (c_0 + c_2) J_n(\alpha) - \frac{c_2}{\pi} \left[J_{n+1}(\alpha) + \frac{n(n-1)}{\pi} J_n(\alpha) \right] \right\} \quad n=1,3,5,\dots \quad (4.15)$$

Similarly, the real part of C_n is

$$C'_n = (-1)^{\frac{n}{2}+2} 2 c_1 \left\{ (n+1) J_n(\alpha) - \pi J_{n+1}(\alpha) \right\} \quad n=0,2,4,\dots \quad (4.16)$$

$$C'_n = (-1)^{\frac{n+3}{2}} 2 \left\{ \left[\pi c_0 + c_2 \left(\pi - \frac{2n}{\pi} - \frac{n(n-1)}{\pi} \right) \right] J_n(\alpha) + c_2 J_{n+1}(\alpha) \right\} \quad n=1,3,5,\dots \quad (4.17)$$

and the imaginary part reduces to

$$C''_n = (-1)^{\frac{n}{2}+1} 2 \left\{ \left[\pi c_0 + c_2 \left(\pi - \frac{2n}{\pi} - \frac{n(n-1)}{\pi} \right) \right] J_n(\alpha) + c_2 J_{n+1}(\alpha) \right\} \quad n=0,2,4,\dots \quad (4.18)$$

$$C''_n = (-1)^{\frac{n+3}{2}} 2 c_1 \left\{ (n+1) J_n(\alpha) - \pi J_{n+1}(\alpha) \right\} \quad n=1,3,5,\dots \quad (4.19)$$

Next we discuss the calculation of the A_n coefficients. From equation (3.34) there results

$$A'_n = C'_n - \kappa B''_n \quad , \quad (4.20)$$

and

$$A_n'' = C_n'' + \kappa B_n' . \quad (4.21)$$

4.2 Solution of the Algebraic Equations

The set of N complex algebraic equations given by

$$a_m = \sum_{n=0}^N \tilde{C}_{mn} a_n + r_m ; \quad m = 0, 1, 2, \dots, N$$

is separated into two sets, using the following notation:

$$\tilde{C}_{mn} = \tilde{C}_{mn}' + i \tilde{C}_{mn}'' \quad (4.22)$$

$$r_m = r_m' + i r_m'' . \quad (4.23)$$

We obtain

$$a_m' = \sum_{n=0}^N (\tilde{C}_{mn}' a_n' - \tilde{C}_{mn}'' a_n'') + r_m' ; \quad m = 0, 1, 2, \dots, N \quad (4.24)$$

$$a_m'' = \sum_{n=0}^N (\tilde{C}_{mn}'' a_n' + \tilde{C}_{mn}' a_n'') + r_m'' ; \quad m = 0, 1, 2, \dots, N \quad (4.25)$$

To solve these equations for the a_n' and a_n'' , we use an iterative method, whereby we assume some arbitrary values for the unknowns in the first equation of the first set and compute an initial value for the first unknown to the left of the equation. This value will be used in the second equation and so on until initial values of the first $2N$ unknowns are found. Then the equations are solved again for a second set of values for the $2N$ unknowns, making use of the first set

for starting values. This procedure is continued until the difference between values for the unknowns obtained from two successive iterations is less than some preassigned value. The computer program used for this operation is designed to provide this check for accuracy in solving the equations. This iteration method was found to be effective for computing the A_n' and A_n'' for all values of the reduced frequency greater than the critical frequency. For frequencies in the range $0 \leq k < k_{\text{critical}}$, the method fails. This failure is noted for depths that are small compared to the half-chord only. The method is satisfactory for all frequencies at large depths. Note that k_{critical} is the value of k for which no solution exists.

For the range $0 \leq k < k_{\text{critical}}$ and for $D < 4$, the Crout method [27] was used to obtain a solution for the equations. The Crout method will give satisfactory results for all frequencies, but is somewhat slower in regard to computer time than the iterative procedure described above.

All calculations were done by utilizing a high-speed digital computer. Values for the real and imaginary parts of the B_n and C_n coefficients are given in Table 2. These coefficients are not functions of the reduced frequency k as are the A_n coefficients. The A_n values can be obtained through the simple relations (4.20) and (4.21) and are not tabulated here.

TABLE 2

REAL AND IMAGINARY PARTS OF B_n AND C_n

n	B_n'	B_n''	C_n'	C_n''
0	-0.04084412	-0.02390768	-0.10066456	0.08960791
1	0.03316639	0.02193889	0.12262104	-0.08028761
2	-0.04143261	0.00205140	-0.03433178	0.13348571
3	0.01402839	-0.02095180	-0.04310939	-0.07208199
4	0.00361431	0.01181532	0.04983858	0.00888488
5	-0.00574890	-0.00155564	-0.01419494	0.02244056
6	0.00142237	-0.00204627	-0.00765042	-0.00778154
7	0.00058169	0.00061490	0.00287355	-0.00211474
8	-0.00019193	0.00013840	0.00049327	0.00082705
9	-0.00002839	-0.00004819	-0.00019737	0.00009970
10	0.00001023	-0.00000513	-0.00001779	-0.00004045
11	0.00000083	0.00000189	0.00000728	-0.00000284

Note: $\alpha = \pi$, $c_0 = 0.023$, $c_1 = 0.042$, $c_2 = 0.034$.

4.3 The Resulting Thrust

The thrust coefficient at infinite depth is independent of the flow velocity U as shown in Appendix C. For finite depths ($D < 4$) the flow velocity enters the calculations through the Froude number. As the time required for the execution of the computer program is fairly great, only one flow velocity was considered. All the results reported here are for a flow velocity of $U = 3$ units per second.

With the Q_n , B_n , and C_n in hand, the thrust coefficient may be computed from equations (3.60) and (3.61). The first attempt to calculate the thrust coefficient was made using a depth of $D = 50.0$. It was

correctly presumed that this depth was large enough to simulate an infinite running depth. The results obtained are shown in Table 3 and Figure 5. Also listed in Table 3 are the results obtained by Siekmann [8]. The infinite sums involved in the expression for the thrust were found to converge fairly rapidly so that six of the α_n gave results comparable to those obtained by Siekmann at an infinite depth. The first six α_n were computed to within 1 per cent accuracy. Looking at equation (3.60) for the time average value of the thrust, it is seen that the last two sums involve only the first two α_n , but an infinite number of the B_n . As the B_n are fairly easy to calculate and require little computer time, these two sums are evaluated for $n = 11$. For higher n , the B_n are so small that their contribution is negligible.

Several attempts were made, using successively smaller depths beginning with $D = 2.0$. Some differences were noted in the thrust coefficient for depths just below 1.0, but the depth must be smaller than this for a clearly discernible deviation from the thrust at infinite depth to be observed. Indeed, to register the effect of the free surface waves on the thrust for the full range of reduced frequencies of interest, it was necessary to decrease the depth to as little as $D = 1/4$. The results for this depth and for several values of the reduced frequency are shown in Table 4 and Figure 5.

The asymptotic behavior of the thrust in the neighborhood of the critical frequency requires the observation that in the interest of

TABLE 3
THRUST COEFFICIENT
 $\alpha = \pi$, $D = 50.0$ and ∞

k	$D = \infty$	$D = 50.0$
0.00	0.000016	0.000
0.20	-0.003408	0.100
0.40	-0.004223	0.250
0.60	-0.004451	0.350
0.80	-0.004466	0.500
1.00	-0.004368	0.650
2.00	-0.003040	0.750
3.00	-0.000674	0.893
4.00	0.002650	0.900
5.00	0.006923	2.000
6.00	0.012143	3.000
7.00	0.018311	4.000
8.00	0.025425	6.000
9.00	0.033486	8.000
10.00	0.042495	10.000

TABLE 4

THRUST COEFFICIENT
 $\alpha = \pi$

k	$D = 1/4$
0.00	-0.016786
0.20	-0.017204
0.40	-0.018161
0.60	-0.017548
0.80	-0.014993
1.00	-0.011883
2.00	-0.003925
3.00	-0.007620
4.00	-0.007836
5.00	-0.003677
6.00	-0.001277
7.00	0.001536
8.00	0.009904
9.00	0.019798
10.00	0.032282

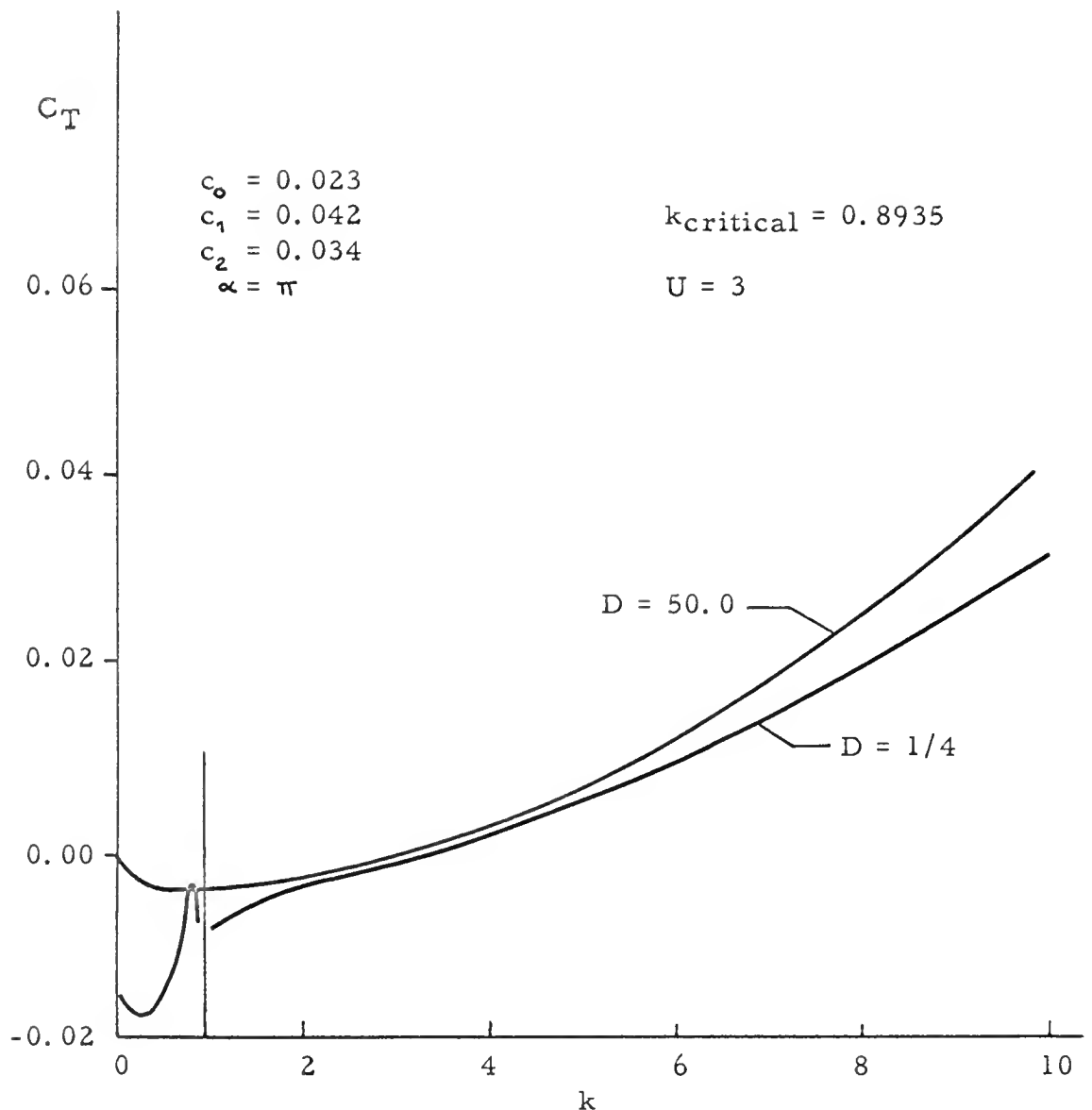


Figure 5. Thrust Coefficient Versus Reduced Frequency

forward motion with as little effort as possible, the "fish" had best not swim at this frequency. This singular phenomenon also indicates that a hydrofoil experiencing vibration with an infinite number of degrees of freedom at just the right frequency might expect to encounter a high drag coefficient for the proper flow velocity. Again, note that the critical frequency is a function of the flow velocity alone. It is not a function of the depth.

The interaction of complicated wave trains on the surface provides an interesting oscillatory behavior for the thrust coefficient at frequencies in the range of $0 \leq k < k_{\text{critical}}$. This effect is shown separately in Figure 6 where the scale has been lengthened. Note also the wave drag [28] for zero frequency. At infinite or large depth the thrust is zero at zero frequency, as required by D'Alembert's paradox.

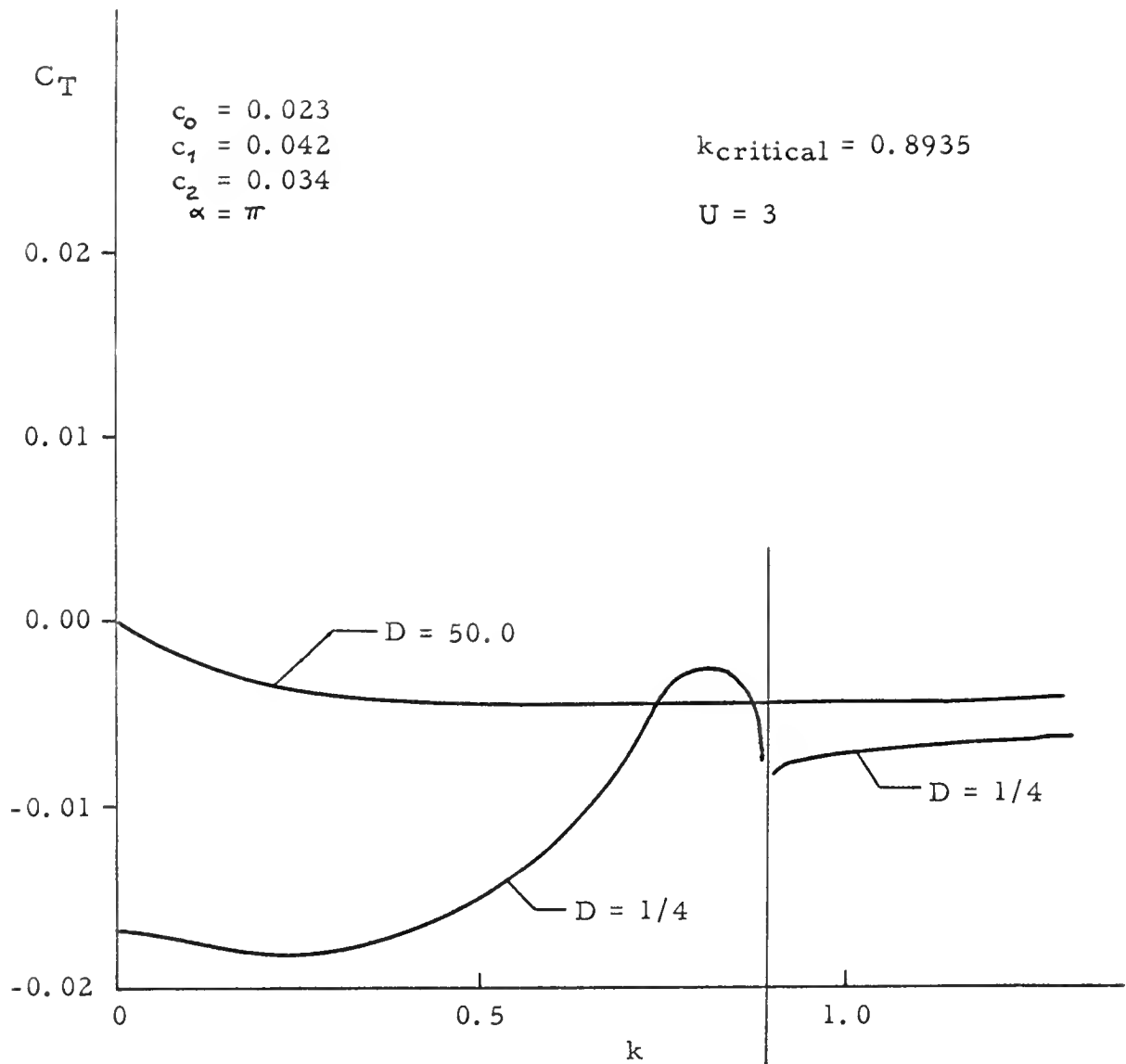


Figure 6. Thrust Coefficient Versus Reduced Frequency
for Small Reduced Frequencies

CHAPTER V

SUMMARY AND CONCLUSIONS

In this study the influence of free surface waves on the swimming of a thin, flexible, two-dimensional, oscillating plate was investigated. The motion of the plate was assumed to approximate the swimming action of a thin flat fish near the free surface of a body of water. The fluid was assumed to be perfect and infinitely deep.

The propulsive effect is due to the motion of the plate, consisting of traveling waves emanating from the "fish" nose which move toward the tail with increasing amplitude. The waves are harmonic with respect to time.

The "fish" is replaced with a mathematical model consisting of a vortex sheet of harmonically varying strength. Such a model requires that vortices be shed from the tail of the plate and carried downstream with the flow. These wake vortices are adequately taken into account by the theory presented. The assumption that they always lie in the plane of the oscillating plate simplifies the theory, but it is still an open question as to whether this assumption is the correct one. Actually, photographs of an oscillating model indicate that the wake vortices deviate in their downstream path from the plane of the plate

by perhaps as much as a quarter of the chord at a distance of only a chord length behind the plate. Taking into account the fact that the vortices in the wake are discharged at the tail of the plate with a velocity vector which is not in alignment with the free stream velocity means that the vortices will continue to diverge from the plane of the plate, or $y = 0$.

In addition to the plate system of vortices and its wake, an image system identical to the plate system was postulated to lie just above the surface so as to make the effect of the whole model on the surface null. This sort of model was postulated to allow the use of an exact potential theory. The velocity potential of the plate system and its image was written down in terms of their unknown vortex strength distribution. Then a third potential function was introduced which took into account the free surface waves. This function was investigated through a partial differential equation resulting from the application of the free surface boundary conditions. Finally, the boundary condition concerning the impenetrability of the oscillating plate was used to obtain an integral equation for the vortex strength distribution. The integral equation was solved by the assumption that the vortex strength distribution could be represented by a Glauert trigonometric series. This introduced a system of infinite algebraic equations. The pressure distribution and the thrust coefficient are

functions of the solution to this system of equations. The equations were solved by the approximate scheme of truncating the set and solving repeatedly while increasing the number of equations solved until values for the first N unknowns become apparent. The thrust coefficient was then evaluated for a flow velocity of $U = 3$ and several different depths.

The results of the calculations for a quadratically varying amplitude function with coefficients which are thought to approximate the swimming of a fish indicate the following conclusions.

1. The theory produces accurate results for the thrust coefficient versus reduced frequency variation for a depth ($D = 50.0$) large enough to simulate an infinite depth when compared to figures obtained by a different method.

2. The influence of the free surface is not a marked factor for relatively shallow depths. One must decrease the running depth to about one-fourth the half-chord in order to note a finite difference in the thrust from that observed at an infinite depth.

3. The influence of the free surface waves causes a varying difference in the thrust coefficient. At high reduced frequencies the difference is greater than at low frequencies, provided k is greater than the critical frequency. At frequencies between zero and the critical frequency the thrust (or in this case, drag) coefficient varies in an

oscillatory manner. The point of zero thrust does not occur at a reduced frequency equal to the wave number of the plate motion, but at a slightly higher value for small depths.

4. As a natural consequence of the theory used for this study, the wave drag for zero reduced frequency is obtained without difficulty. This might be of interest to designers working in the field of hydrofoil craft equipped with slightly bent wings.

APPENDIXES

APPENDIX A

THE FREE SURFACE POTENTIAL

To solve the partial differential equation

$$\frac{\partial^2 \Phi_3}{\partial x^2} + 2ik \frac{\partial \Phi_3}{\partial x} + \frac{1}{F^2} \frac{\partial \Phi_3}{\partial y} - k^2 \Phi_3 = \frac{1}{\pi F^2} \int_{-1}^1 \frac{\gamma(\xi)(x-\xi)}{(x-\xi)^2 + D^2} d\xi -$$

$$- \frac{ik\bar{\Gamma}}{\pi F^2} \int_1^\infty \frac{e^{-ik(\xi-1)} (x-\xi)}{(x-\xi)^2 + D^2} d\xi, \quad (A1)$$

we proceed as follows, using the operator notation

$$\mathcal{D} = \frac{\partial}{\partial x}, \quad \mathcal{D}' = \frac{\partial}{\partial y}. \quad (A2)$$

A particular integral of (A1) is written in symbolic form as

$$\begin{aligned} {}^p \Phi_3 &= \frac{1}{\mathcal{A}(\mathcal{D}, \mathcal{D}')} \left\{ \frac{1}{\pi F^2} \int_{-1}^1 \frac{\gamma(\xi)(x-\xi)}{(x-\xi)^2 + D^2} d\xi - \right. \\ &\quad \left. - \frac{ik\bar{\Gamma}}{\pi F^2} \int_1^\infty \frac{e^{-ik(\xi-1)} (x-\xi)}{(x-\xi)^2 + D^2} d\xi \right\}, \end{aligned} \quad (A3)$$

where

$$\mathcal{A}(\mathcal{D}, \mathcal{D}') = \mathcal{D}^2 + 2ik\mathcal{D} + \frac{1}{F^2} \mathcal{D}' - k^2. \quad (A4)$$

Now it can be established that

$$\frac{x-\xi-i(y-2D)}{(x-\xi)^2+(y-2D)^2} = i \int_0^\infty e^{-is[x-\xi+i(y-2D)]} ds, \quad y-2D < 0. \quad (A5)$$

Then it follows that

$$\begin{aligned} \frac{x-\xi}{(x-\xi)^2+(y-2D)^2} &= \operatorname{Re} \left\{ i \int_0^\infty e^{s(y-2D)} e^{-is(x-\xi)} ds \right\} \\ &= \int_0^\infty e^{s(y-2D)} \sin s(x-\xi) ds \\ &= \frac{1}{2i} \int_0^\infty e^{s(y-2D)} \left[e^{is(x-\xi)} - e^{-is(x-\xi)} \right] ds, \quad (A6) \end{aligned}$$

and that the particular integral ${}^p\Phi_3$ may be written symbolically as

(see [29, p. 103])

$$\begin{aligned} {}^p\Phi_3 &= \frac{1}{\mathcal{H}(\mathfrak{D}, \mathfrak{D}')} \left\{ \frac{1}{2i\pi F^2} \int_{-1}^1 \chi(\xi) \int_0^\infty e^{s(y-2D)} \left[e^{is(x-\xi)} - e^{-is(x-\xi)} \right] ds d\xi - \right. \\ &\quad \left. - \frac{\kappa \bar{P}}{2\pi F^2} \int_1^\infty e^{-ik(\xi-1)} \int_0^\infty e^{s(y-2D)} \left[e^{is(x-\xi)} - e^{-is(x-\xi)} \right] ds d\xi \right\}. \quad (A7) \end{aligned}$$

We also observe that for an equation like

$$\mathcal{H}(\mathfrak{D}, \mathfrak{D}') \varphi = e^{ax+by},$$

the particular solution consists of terms of the type

$${}^p\varphi = \frac{1}{\mathcal{H}(a, b)} e^{ax+by},$$

so that the particular integral ${}^p\Phi_3$ may be written as

$$\begin{aligned} {}^p\Phi_3 = & \frac{i}{2\pi F^2} \int_{-1}^1 \gamma(\xi) G_p(x, y; \xi) d\xi + \\ & + \frac{\kappa \bar{\Gamma}}{2\pi F^2} \int_1^\infty e^{-iK(\xi-1)} G_p(x, y; \xi) d\xi, \end{aligned} \quad (A8)$$

where

$$G_p(x, y; \xi) = \int_0^\infty e^{s(y-zD)} \left[\frac{e^{is(x-\xi)}}{(s-s_1)(s-s_2)} - \frac{e^{-is(x-\xi)}}{(s-s_3)(s-s_4)} \right] ds,$$

and

$$(s-s_1)(s-s_2) = s^2 - \left(\frac{1}{F^2} - 2K \right) + K^2,$$

$$(s-s_3)(s-s_4) = s^2 - \left(\frac{1}{F^2} + 2K \right) + K^2.$$

For the complementary solution we write (see [29, p. 102])

$${}^c\Phi_3 = \frac{i}{2\pi F^2} \int_{-1}^1 \gamma(\xi) G_c(x, y; \xi) d\xi + \frac{\kappa \bar{\Gamma}}{2\pi F^2} \int_1^\infty e^{-iK(\xi-1)} G_c(x, y; \xi) d\xi, \quad (A9)$$

where

$$\begin{aligned} G_c(x, y; \xi) = & D_1 e^{[y-zD+i(x-\xi)]s_1} + D_2 e^{[y-zD+i(x-\xi)]s_2} + \\ & + D_3 e^{[y-zD-i(x-\xi)]s_3} + D_4 e^{[y-zD-i(x-\xi)]s_4}, \end{aligned}$$

and the S_j are defined as in (A8). Upon adding (A8) and (A9), the general solution of the partial differential equation (A1) appears as it is given by equation (1.44) in Chapter I.

To fix the values of the constants D_j , we proceed as follows:

If a small dissipative force

$$-\mu \text{ grad } \Phi \quad (\text{A10})$$

is introduced into the analysis, the external force potential Ω in equation (1.16) becomes

$$\Omega = g\eta + \mu\Phi. \quad (\text{A11})$$

This leaves the Laplace equation

$$\nabla^2 \Phi = 0 \quad (\text{A12})$$

unaltered, but makes the boundary condition given by (1.41) become

$$\Phi_{tt} + 2U\Phi_{xt} + U^2\Phi_{xx} + \mu U\Phi_x + \mu\Phi_t + g\Phi_y = 0, \quad y=0. \quad (\text{A13})$$

Substituting from equations (1.38), (1.39), and (1.40) into (A13), we get

$$\begin{aligned} \frac{\partial^2 \Phi_3}{\partial x^2} + 2K(\beta + i) \frac{\partial \Phi_3}{\partial x} + \frac{1}{F^2} \frac{\partial \Phi_3}{\partial y} + K^2(2i\beta - 1) \Phi_3 = \\ \frac{1}{\pi F^2} \int_{-1}^1 \frac{g(\xi)(x-\xi)}{(x-\xi)^2 + D^2} d\xi - \frac{iK\bar{F}}{\pi F^2} \int_1^\infty \frac{e^{-iK(F-1)} (x-\xi)}{(x-\xi)^2 + D^2} d\xi, \end{aligned} \quad (\text{A14})$$

which governs the behavior of the spatial portion $\Phi_3(x, y)$ of the free surface potential $\Phi_3(x, y, t)$. In equation (A14) the Froude number F , the reduced frequency k , and a new parameter β , related to the dissipative coefficient μ , are as follows:

$$F = \frac{U}{\sqrt{g}}, \quad K = \frac{\omega}{U}, \quad \beta = \frac{\mu}{2\omega}.$$

A particular integral of (A14) is obtained just as for the partial differential equation (A1) already treated. However, the function $G(x, y; \xi)$ of equation (A8) evaluated on the free surface $y = D$ becomes

$$\bar{G}(x, D; \xi) = \int_0^\infty e^{-Ds} \left[\frac{e^{is(x-\xi)}}{(s-\sigma_1)(s-\sigma_2)} - \frac{e^{-is(x-\xi)}}{(s-\sigma_3)(s-\sigma_4)} \right] ds, \quad (A15)$$

where

$$(s-\sigma_1)(s-\sigma_2) = s^2 - \left[\frac{1}{F^2} - z\kappa(1-i\beta) \right] s + \kappa^2(1-z^2\beta^2),$$

$$(s-\sigma_3)(s-\sigma_4) = s^2 - \left[\frac{1}{F^2} + z\kappa(1-i\beta) \right] s + \kappa^2(1-z^2\beta^2).$$

As both the integrals in (A15) are singular at σ_j , Cauchy principal values must be considered. The σ_j are given by

$$\sigma_{1,2} = \frac{1}{2F^2} \left[1 - z\kappa F^2(1-i\beta) \pm (1 - 4\kappa F^2 + 4i\beta\kappa F^2 - 4\kappa^2 F^4 \beta^2)^{\frac{1}{2}} \right], \quad (A16)$$

and

$$\sigma_{3,4} = \frac{1}{2F^2} \left[1 + z\kappa F^2(1-i\beta) \pm (1 + 4\kappa F^2 - 4i\beta\kappa F^2 - 4\kappa^2 F^4 \beta^2)^{\frac{1}{2}} \right]. \quad (A17)$$

When $\beta = 0$, the roots $\sigma_{1,2}$ and $\sigma_{3,4}$ become

$$s_{1,2} = \frac{1}{2F^2} \left[1 - z\kappa F^2 \pm (1 - 4\kappa F^2)^{\frac{1}{2}} \right], \quad (A18)$$

and

$$s_{3,4} = \frac{1}{2F^2} \left[1 + z\kappa F^2 \pm (1 + 4\kappa F^2)^{\frac{1}{2}} \right]. \quad (A19)$$

Now it is the behavior of the roots σ_j when $\beta \rightarrow 0$ which is critical to this analysis. Upon examining equations (A16) and (A17) as $\beta \rightarrow 0$, the results in Table 5 are indicated.

TABLE 5

VARIATION OF σ_j , $j = 1, 2, 3, 4$, WITH kF^2

kF^2	Real				Imaginary			
	σ_1	σ_2	σ_3	σ_4	σ_1	σ_2	σ_3	σ_4
0	$1/F^2$	0	$1/F^2$	0	0+	0	0-	0
$0 < kF^2 < 1/4$	(+)	(+)	(+)	(+)	0+	0-	0-	0-
$1/4 < kF^2 < 1/2$	(+)	(+)	(+)	(+)	(+)	(-)	0-	0-
$1/2 < kF^2 < \infty$	(-)	(-)	(+)	(+)	(+)	(-)	0-	0-

Notes:

These results may be found in Tan's paper [16] except for an error which has been corrected here. Tan indicated that $\lim_{\beta \rightarrow 0} \Im \sigma_2 = 0+$ for $0 < kF^2 < 1/4$. This led him to the conjecture that no waves could exist upstream of the disturbance, or in this case the plate.

The notation "0+" or "0-" indicates that as $\beta \rightarrow 0$, the imaginary part of the root indicated approaches the real axis from the positive or negative side respectively.

Return now to the integral in (A15). By writing

$$\frac{1}{(s-\sigma_1)(s-\sigma_2)} = \frac{1}{\sigma_1 - \sigma_2} \left[\frac{1}{s-\sigma_1} - \frac{1}{s-\sigma_2} \right], \quad (A20)$$

and doing the same for the term involving σ_3 and σ_4 , we may write the function $\bar{G}(x, D; \xi)$ as

$$\tilde{G}(x, 0; \xi) = \frac{1}{\sigma_1 - \sigma_2} \left[I_1' - I_2' \right] - \frac{1}{\sigma_3 - \sigma_4} \left[I_3' - I_4' \right] , \quad (A21)$$

where

$$I_j' = \int_0^\infty \frac{e^{[-\sigma + i(x-\xi)]s}}{s - \sigma_j} ds ; \quad j = 1, 2 \quad (A22)$$

$$I_j' = \int_0^\infty \frac{e^{[-\sigma - i(x-\xi)]s}}{s - \sigma_j} ds ; \quad j = 3, 4 . \quad (A23)$$

These integrals may be evaluated by contour integration in the complex $z = s + im$ plane and use of Cauchy's integral theorem. The proper contours must be chosen with care. Due to the term $e^{-\sigma s}$ in the integrals, no part of the negative S -axis may be used. The choice of the remaining first or fourth quadrants depends on the sign of $(x - \xi)$. This will be evident later. The contours to be used are those shown in Figure 7.

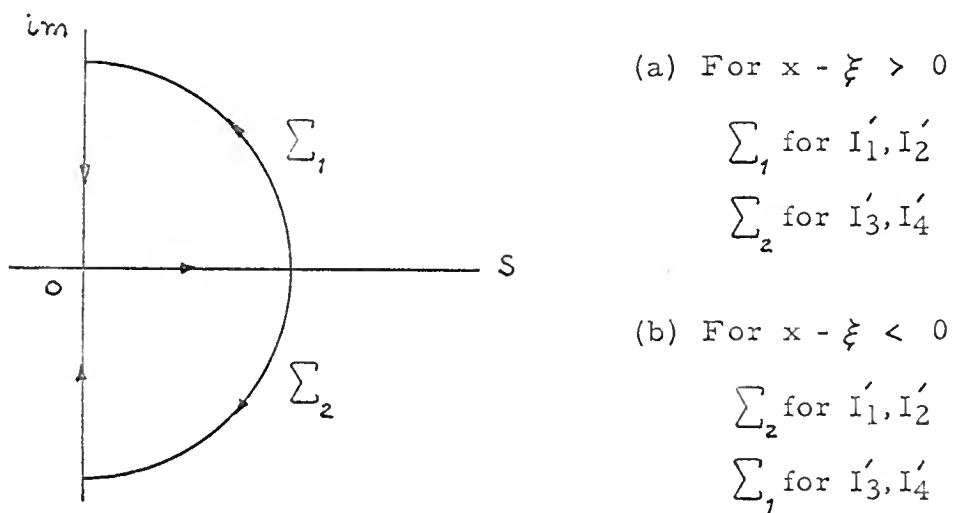


Figure 7. Contours of Integration for the I_j' Integrals, $j = 1, 2, 3, 4$

When a pole corresponding to σ_j lies inside the contour of integration, the result obtained using Cauchy's integral theorem includes the residue at this pole. As we will see later, by allowing x to approach $\pm\infty$, these residue terms are responsible for harmonic wave trains which propagate to infinity.

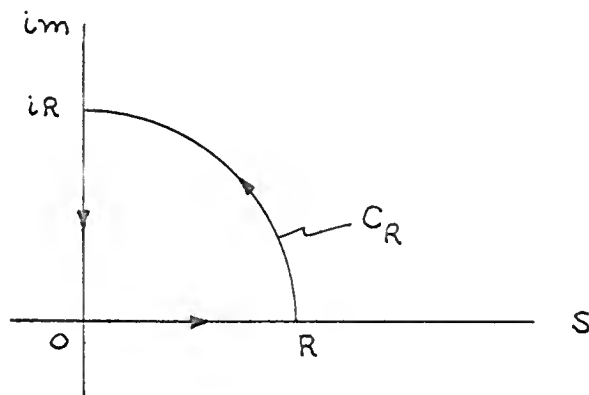


Figure 8. Contour of Integration for I_1'

As an example of the integration procedure, consider I_1' for the range $x - \xi > 0$. According to the scheme in Figure 7, the contour \sum , is to be used in this case. Integrating around this contour, shown in Figure 8, and using Cauchy's integral formula, we have

$$\begin{aligned}
 & \int_0^R \frac{e^{[-D+i(x-\xi)]s}}{s - \sigma_j} ds + \int_{C_R} \frac{e^{[-D+i(x-\xi)]z}}{z - \sigma_j} dz - \\
 & - \int_0^R \frac{e^{[-D+i(x-\xi)]im}}{m + i\sigma_j} dm = 2\pi i e^{[-D+i(x-\xi)]\sigma_j} , \quad (A24)
 \end{aligned}$$

where it has been assumed that σ_1 does lie within the contour \sum_1 .

In order for this to be so, the real part and the imaginary part of σ_1 must be positive. Whether or not this is true may be ascertained from Table 5. Now, allow R to approach ∞ in equation (A24). The second integral can be shown to vanish: We observe that

$$\begin{aligned} \left| e^{-Dz} \right| &= \left| e^{-D(s+im)} \right| = e^{-Ds} < 1 \quad \text{for} \quad \frac{s}{D} > 0, \\ \left| e^{i(x-\xi)z} \right| &= \left| e^{-aR \sin \theta} \right|, \end{aligned}$$

and if R is sufficiently large,

$$\left| \frac{1}{z - \sigma_1} \right| < \delta,$$

so that

$$\left| \int_{C_R} \frac{e^{[-D+i(x-\xi)]z}}{z - \sigma_1} dz \right| < \delta R \int_0^{\pi/2} e^{-aR \sin \theta} d\theta, \quad (A25)$$

where $a = x - \xi$. Now

$$\frac{\sin \theta}{\theta} \geq \frac{2}{\pi}, \quad 0 \leq \theta \leq \frac{\pi}{2},$$

so that

$$\left| \int_{C_R} \frac{e^{-Dz} e^{i(x-\xi)z}}{z - \sigma_1} dz \right| < \delta R \int_0^{\pi/2} e^{-\frac{zaR\theta}{\pi}} d\theta = \frac{\delta \pi}{za} \left[1 - e^{-aR} \right] < \frac{\delta \pi}{za},$$

and as $\delta \rightarrow 0$ for $R \rightarrow \infty$, the integral clearly vanishes. Thus, we obtain from (A24)

$$I'_1 = 2\pi i e^{[-D+i(x-\xi)]\sigma_1} + \int_0^\infty \frac{e^{[-D+i(x-\xi)]im}}{m + i\sigma_1} dm.$$

Proceeding in the same manner, taking care to observe the proper contours of integration, we obtain similar results for I_2' , I_3' , and I_4' for the case $x - \xi > 0$:

$$I_j' = 2\pi i e^{[-D+i(x-\xi)]\sigma_j} + \int_0^\infty \frac{e^{[-D+i(x-\xi)]im}}{m+i\sigma_j} dm ; j=1,2 \quad (A26)$$

$$I_j' = -2\pi i e^{[-D-i(x-\xi)]\sigma_j} + \int_0^\infty \frac{e^{[-D-i(x-\xi)](-im)}}{m-i\sigma_j} dm ; j=3,4. \quad (A27)$$

For $x - \xi < 0$, or upstream from the plate, we obtain

$$I_j' = -2\pi i e^{[D+i(x-\xi)]\sigma_j} + \int_0^\infty \frac{e^{[D+i(x-\xi)](-im)}}{m-i\sigma_j} dm ; j=1,2 \quad (A28)$$

$$I_j' = 2\pi i e^{[-D-i(x-\xi)]\sigma_j} + \int_0^\infty \frac{e^{[-D-i(x-\xi)]im}}{m+i\sigma_j} dm ; j=3,4. \quad (A29)$$

Since what is sought are the flow conditions at infinity, the next step is to note that the definite integrals in equations (A26), (A27), (A28), and (A29) decrease rapidly for large $x - \xi$. Thus, they contribute only local disturbances around the plate. Further, note that an infinite propagation of waves can occur only when

$$\lim_{\beta \rightarrow 0} \operatorname{Im} \sigma_j = 0^\pm ,$$

and even then a wave results only when the σ_j is contained in the contour of integration.

It is helpful to write a compilation of the results for $\bar{G}(x, D; \xi)$ as $x \rightarrow \pm \infty$. This is shown in Table 6. A reminder of the contour of integration used for each integral making a contribution to \bar{G} is also included in the table.

It is a simple matter now to compile the values of \bar{G}_+ and \bar{G}_- for the ranges of the flow parameter kF^2 , i.e., from Tables 5 and 6 we have

(a) For $kF^2 = 0$

$$\begin{aligned}\bar{G}_+ &= \frac{2\pi i}{\sigma_1} e^{[-D+i(x-\xi)]\sigma_1} + \frac{2\pi i}{\sigma_3} e^{[-D+i(x-\xi)]\sigma_3}, \\ \bar{G}_- &= 0.\end{aligned}\quad (A30)$$

(b) For $0 < kF^2 < 1/4$

$$\begin{aligned}\bar{G}_+ &= \frac{2\pi i}{\sigma_1 - \sigma_2} e^{[-D+i(x-\xi)]\sigma_1} + \frac{2\pi i}{\sigma_2 - \sigma_4} \left[e^{[-D-i(x-\xi)]\sigma_3} - e^{[-D-i(x-\xi)]\sigma_4} \right], \\ \bar{G}_- &= \frac{2\pi i}{\sigma_1 - \sigma_2} e^{[-D+i(x-\xi)]\sigma_2}.\end{aligned}\quad (A31)$$

(c) For $1/4 < kF^2 < 1/2$

$$\begin{aligned}\bar{G}_+ &= \frac{2\pi i}{\sigma_3 - \sigma_4} \left[e^{[-D-i(x-\xi)]\sigma_3} - e^{[-D-i(x-\xi)]\sigma_4} \right], \\ \bar{G}_- &= 0.\end{aligned}\quad (A32)$$

(d) For $1/2 < kF^2 < \infty$

$$\begin{aligned}\bar{G}_+ &= \frac{2\pi i}{\sigma_3 - \sigma_4} \left[e^{[-D-i(x-\xi)]\sigma_3} - e^{[-D-i(x-\xi)]\sigma_4} \right], \\ \bar{G}_- &= 0;\end{aligned}\quad (A33)$$

for $\bar{G}(x, D; \xi)$ we are to write

$$\bar{G} = \bar{G}_+ + \bar{G}_-. \quad (A34)$$

TABLE 6

 $\bar{G}(x, D; \xi)$ FOR $x \rightarrow \pm \infty$

$\bar{G}_+ = \frac{2\pi i}{\sigma_1 - \sigma_2} \left\{ e^{[-D + i(x - \xi)]\sigma_1} - e^{[-D + i(x - \xi)]\sigma_2} \right\} + \frac{2\pi i}{\sigma_3 - \sigma_4} \left\{ e^{[-D - i(x - \xi)]\sigma_3} - e^{[-D - i(x - \xi)]\sigma_4} \right\}$ <p style="text-align: center;">$x \rightarrow +\infty$ (Downstream)</p> 	$\bar{G}_- = \frac{-2\pi i}{\sigma_1 - \sigma_2} \left\{ e^{[-D + i(x - \xi)]\sigma_1} - e^{[-D + i(x - \xi)]\sigma_2} \right\} - \frac{2\pi i}{\sigma_3 - \sigma_4} \left\{ e^{[-D - i(x - \xi)]\sigma_3} - e^{[-D - i(x - \xi)]\sigma_4} \right\}$ <p style="text-align: center;">$x \rightarrow -\infty$ (Upstream)</p> 
---	---

It would appear that for the range $1/4 < kF^2 < 1/2$ another wave train should be included since both σ_1 and σ_2 lie within the accepted contours of integration. However, $\lim_{\beta \rightarrow 0} \operatorname{Im} \sigma_{1,2} \neq 0$, and the resulting wave trains are damped out as $x \rightarrow \pm\infty$. For example, suppose σ_1 is written as

$$\sigma_1 = \alpha_1 + i\gamma_1 \quad ; \quad \alpha_1, \gamma_1 > 0.$$

The corresponding \bar{G} contribution would be

$$\begin{aligned} \bar{G}_+ &= \frac{z\pi i}{(\alpha_1 + i\gamma_1) - \sigma_2} \left\{ e^{[-D + i(x-\xi)](\alpha_1 + i\gamma_1)} \right\} \\ &= \frac{z\pi i}{(\alpha_1 + i\gamma_1) - \sigma_2} e^{i[-D\gamma_1 + \alpha_1(x-\xi)]} e^{-D\alpha_1 - \gamma_1(x-\xi)}, \end{aligned}$$

and as $x \rightarrow +\infty$, the contribution damps out. The same argument holds for σ_2 in this range of kF^2 . Hence, the two ranges, $1/4 < kF^2 < 1/2$ and $1/2 < kF^2 < \infty$, could just as well be considered as one range, i.e., $1/4 < kF^2 < \infty$ as far as the final results are concerned.

Now consider the function $G(x, D; \xi)$ as it is written from equation (1.44b). Again using partial fractions, this function may be written as

$$\begin{aligned} G(x, D; \xi) &= \frac{1}{S_1 - S_2} \left(\bar{I}_1 - \bar{I}_2 \right) - \frac{1}{S_3 - S_4} \left(\bar{I}_3 - \bar{I}_4 \right) + \\ &+ D_1 e^{[-D + i(x-\xi)]S_1} + D_2 e^{[-D + i(x-\xi)]S_2} + \\ &+ D_3 e^{[-D - i(x-\xi)]S_3} + D_4 e^{[-D - i(x-\xi)]S_4}, \quad (A35) \end{aligned}$$

where

$$\bar{I}_j = \int_0^\infty \frac{e^{[-D+i(x-\xi)]s}}{s - S_j} ds ; \quad j = 1, 2 , \quad (A36)$$

$$\bar{I}_j = \int_0^\infty \frac{e^{[-D-i(x-\xi)]s}}{s - S_j} ds ; \quad j = 3, 4 . \quad (A37)$$

In evaluating the above \bar{I}_j integrals, the same quadrant scheme for contours is adhered to as was used in evaluating the I_j integrals of $\bar{G}(x, D; \xi)$. One exception is made in the form of the contour. It has already been shown that no wave train exists at infinity unless the roots σ_j or S_j are real and positive. Thus, we use contours like those shown in Figure 9 when working with the real positive S_j singularities. A semicircular indentation of radius ϵ is taken about the pole S_j . Again, use of one contour or the other is determined by whether $x - \xi$ is greater than or less than zero.

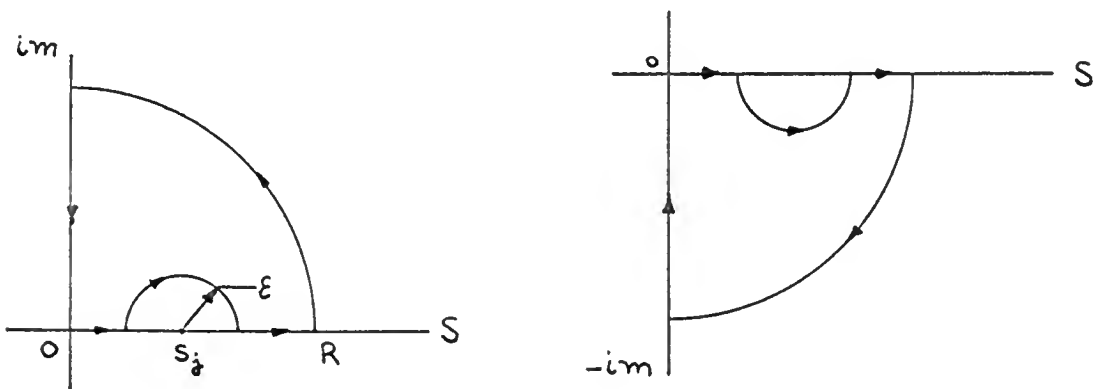


Figure 9. Contours of Integration for \bar{I}_j Integrals, $j = 1, 2, 3, 4$

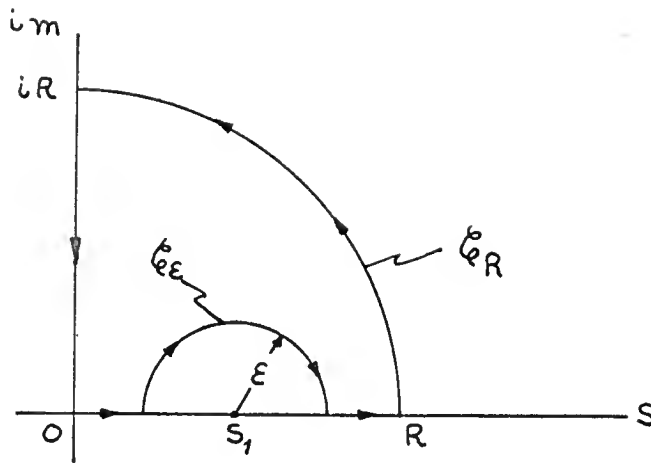


Figure 10. Contour of Integration for \bar{I}_1

As an example of this type of calculation, consider \bar{I}_1 for $x - \xi > 0$. Using the contour shown in Figure 10 and Cauchy's integral formula, we write

$$\begin{aligned}
 & \int_0^{s_1 - \varepsilon} \frac{e^{-[D+i(x-\xi)]s}}{s - s_1} ds + \int_{\xi_\varepsilon} \frac{e^{-[D+i(x-\xi)]z}}{z - s_1} dz + \\
 & \int_{s_1 + \varepsilon}^R \frac{e^{-[D+i(x-\xi)]s}}{s - s_1} ds + \int_{\xi_R} \frac{e^{-[D+i(x-\xi)]z}}{z - s_1} dz - \\
 & -i \int_0^R \frac{e^{-[D+i(x-\xi)]im}}{im - s_1} dm = 0.
 \end{aligned}$$

The fourth integral vanishes as $R \rightarrow \infty$. The first and third integrals combine to give \bar{I}_1 as $R \rightarrow \infty$. The second integral is calculated for $\varepsilon \rightarrow 0$ as follows. On the contour ξ_ε

$$z = \varepsilon e^{i\theta} + s_1,$$

so that

$$\begin{aligned} \int_{\xi-\epsilon}^{\xi} &= -i \int_{-\pi}^0 e^{[-D+i(x-\xi)](s_1+\epsilon e^{i\theta})} d\theta \\ &= -i e^{[-D+i(x-\xi)]s_1} \int_{-\pi}^0 e^{[-D+i(x-\xi)]\epsilon e^{i\theta}} d\theta. \end{aligned}$$

Now we expand the integrand in a Taylor's series like

$$e^{\alpha\epsilon e^{i\theta}} = e^{\alpha\epsilon} + i\alpha\epsilon e^{\alpha\epsilon} \theta + \dots,$$

where $\alpha = -D + i(x - \xi)$. Then

$$\lim_{\epsilon \rightarrow 0} \int_{-\pi}^0 e^{\alpha\epsilon e^{i\theta}} d\theta = \pi,$$

and

$$\lim_{\epsilon \rightarrow 0} \int_{\xi-\epsilon}^{\xi} \frac{e^{[-D+i(x-\xi)]z}}{z-s_1} dz = -\pi i e^{[-D+i(x-\xi)]s_1}.$$

Thus,

$$\bar{I}_1 = \pi i e^{[-D+i(x-\xi)]s_1} + \int_0^\infty \frac{e^{[-D+i(x-\xi)]im}}{m+s_1} dm.$$

As $x \rightarrow +\infty$, the definite integral above diminishes rapidly, and we are left with a result similar to the one obtained for \bar{I}'_1 . The other \bar{I}_j are then calculated for $x - \xi > 0$ and for $x - \xi < 0$. The resulting values are combined according to (A35) and are listed in Table 7.

Again a reminder of the integration contour is provided.

TABLE 7
 $G(x, D; \xi)$ FOR $x \rightarrow \pm \infty$

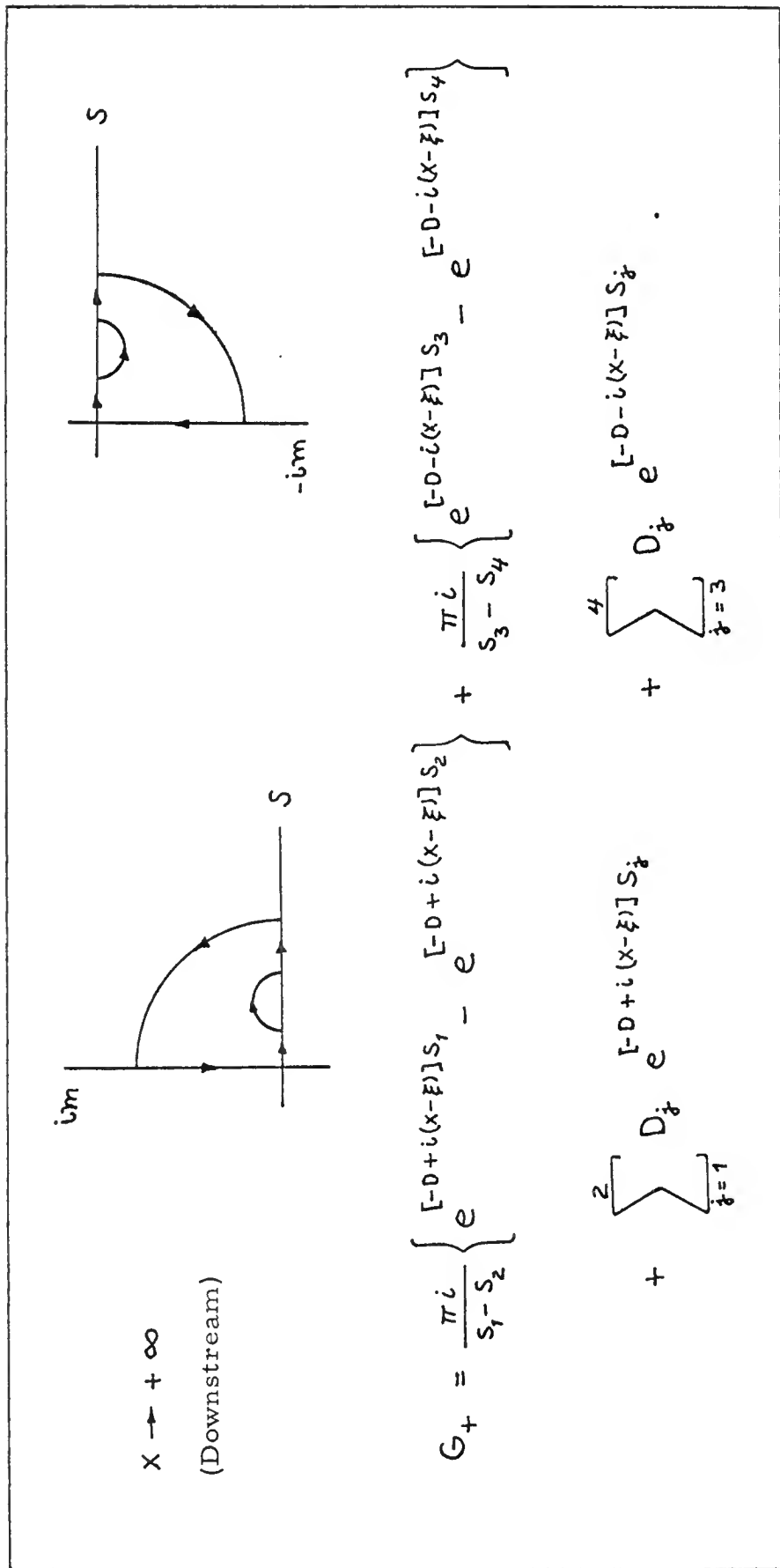
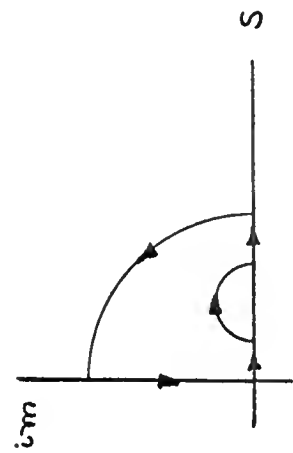
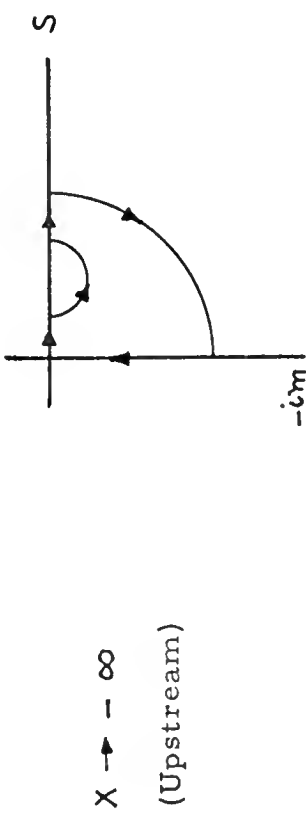


TABLE 7--C Continued



$$G_- = -\frac{\pi i}{s_1 - s_2} \left\{ e^{[-D+i(x-\xi)]s_1} - e^{[-D+i(x-\xi)]s_2} \right\} - \frac{\pi i}{s_3 - s_4} \left\{ e^{[-D-i(x-\xi)]s_3} - e^{[-D-i(x-\xi)]s_4} \right\}$$

$$+ \sum_{\delta=1}^2 D_\delta e^{[-D+i(x-\xi)]s_\delta} + \sum_{\delta=3}^4 D_\delta e^{[-D-i(x-\xi)]s_\delta}$$

Table 8 indicates the behavior of the S_j roots as the flow parameter kF^2 varies.

TABLE 8

VARIATION OF S_j , $j = 1, 2, 3, 4$, WITH kF^2

kF^2	Real				Imaginary			
	S_1	S_2	S_3	S_4	S_1	S_2	S_3	S_4
0	$1/F^2$	0	$1/F^2$	0	0	0	0	0
$0 < kF^2 < 1/4$	(+)	(+)	(+)	(+)	0	0	0	0
$1/4 < kF^2 < 1/2$	(+)	(+)	(+)	(+)	(+)	(-)	0	0
$1/2 < kF^2 < \infty$	(-)	(-)	(+)	(+)	(+)	(-)	0	0

The following compilation indicates the behavior of the $G(x, D; \xi)$ function in an analogous manner to equations (A30), (A31), (A32), (A33), and (A34).

(a) For $kF^2 = 0$

$$G_+ = \frac{\pi i}{S_1} e^{[-D+i(x-\xi)]S_1} + \frac{\pi i}{S_3} e^{[-D+i(x-\xi)]S_3},$$

$$G_- = 0. \quad (A38)$$

(b) For $0 < kF^2 < 1/4$

$$G_+ = \frac{\pi i}{S_1 - S_2} e^{[-D+i(x-\xi)]S_1} + \frac{\pi i}{S_3 - S_4} \left[e^{[-D-i(x-\xi)]S_3} - e^{[-D-i(x-\xi)]S_4} \right],$$

$$G_- = \frac{\pi i}{S_1 - S_2} e^{[-D+i(x-\xi)]S_2}. \quad (A39)$$

(c) For $1/4 < kF^2 < 1/2$

$$G_+ = \frac{\pi i}{S_3 - S_4} \left[e^{[-D - i(x - \xi)]S_3} - e^{[-D - i(x - \xi)]S_4} \right],$$

$$G_- = 0. \quad (A40)$$

(d) For $1/2 < kF^2 < \infty$

$$G_+ = \frac{\pi i}{S_3 - S_4} \left[e^{[-D - i(x - \xi)]S_3} - e^{[-D - i(x - \xi)]S_4} \right],$$

$$G_- = 0, \quad (A41)$$

where $G(x, D; \xi)$ has to be taken as

$$G = G_+ + G_- + \sum_{j=1}^2 D_j e^{[-D + i(x - \xi)]S_j} + \sum_{j=3}^4 D_j e^{[-D - i(x - \xi)]S_j}. \quad (A42)$$

Upon comparing equations (A30) through (A34) with equations (A38) through (A42), the appropriate values of the constants D_j can be assigned. They are as listed in Table 1 of Chapter I.

APPENDIX B

COEFFICIENTS FOR THE INFINITE SET OF EQUATIONS¹

$$\begin{aligned}
 \operatorname{Re}\{\tilde{C}_{\infty}\} = & - \int_0^\infty e^{-20s} J_0(s) \left\{ \left[1 + \frac{s}{F^2} \left(\frac{1}{(s-s_1)(s-s_2)} + \frac{1}{(s-s_3)(s-s_4)} \right) \right] J_1(s) + k \sin s \left[\frac{k}{k^2 - s^2} \right. \right. \\
 & \left. \left. + \frac{s}{F^2} \left(\frac{1}{(k+s)(s-s_1)(s-s_2)} + \frac{1}{(k-s)(s-s_3)(s-s_4)} \right) \right] \right\} ds - k \int_1^\infty \frac{\sin[k(\xi-1)]}{\sqrt{\xi^2-1}} d\xi \\
 & - \frac{\pi}{F^2(s_1-s_2)} \left\{ s_1 e^{-20s_1} J_0(s_1) \left[J_0(s_1) - \frac{k \cos s_1}{k+s_1} \right] + s_2 e^{-20s_2} J_0(s_2) \left[J_0(s_2) - \frac{k \cos s_2}{k+s_2} \right] \right\} \\
 & - \frac{\pi}{F^2(s_3-s_4)} \left\{ s_3 e^{-20s_3} J_0(s_3) \left[J_0(s_3) - \frac{k \cos s_3}{k-s_3} \right] - s_4 e^{-20s_4} J_0(s_4) \left[J_0(s_4) - \frac{k \cos s_4}{k-s_4} \right] \right\} \\
 \operatorname{Im}\{\tilde{C}_{\infty}\} = & \int_0^\infty s e^{-20s} J_0(s) \left\{ \frac{1}{F^2} \left[\frac{1}{(s-s_1)(s-s_2)} - \frac{1}{(s-s_3)(s-s_4)} \right] J_0(s) + k \cos s \left[\frac{1}{k^2 - s^2} \right. \right. \\
 & \left. \left. + \frac{1}{F^2} \left(\frac{1}{(k-s)(s-s_3)(s-s_4)} - \frac{1}{(k+s)(s-s_1)(s-s_2)} \right) \right] \right\} ds - k \int_1^\infty \frac{\cos[k(\xi-1)]}{\sqrt{\xi^2-1}} d\xi \\
 & - \frac{\pi}{F^2(s_1-s_2)} \left\{ s_1 e^{-20s_1} J_0(s_1) \left[J_1(s_1) + \frac{k \sin s_1}{k+s_1} \right] + s_2 e^{-20s_2} J_0(s_2) \left[J_1(s_2) + \frac{k \sin s_2}{k+s_2} \right] \right\} \\
 & + \frac{\pi}{F^2(s_3-s_4)} \left\{ s_3 e^{-20s_3} J_0(s_3) \left[J_1(s_3) + \frac{k \sin s_3}{k-s_3} \right] - s_4 e^{-20s_4} J_0(s_4) \left[J_1(s_4) + \frac{k \sin s_4}{k-s_4} \right] \right\}
 \end{aligned}$$

¹ Terms containing e^{-20s_1} and e^{-20s_2} are omitted when s_1 and s_2 are complex.

$$\operatorname{Re}\{\tilde{C}_{01}\} = -\frac{k}{2} \int_0^\infty e^{-20s} J_0(s) \sin s \left\{ \frac{s}{F^2} \left[\frac{1}{(k-s)(s-s_1)(s-s_2)} + \frac{1}{(k-s)(s-s_3)(s-s_4)} \right] + \frac{k}{k^2-s^2} \right\} ds$$

$$- \frac{k}{2} \int_1^\infty \frac{\sin[k(\xi-1)]}{\sqrt{\xi^2-1}} d\xi$$

$$- \frac{\pi}{F^2(s_1-s_2)} \left\{ e^{-20s_1} J_0(s_1) \left[J_1(s_1) - \frac{k s_1 \cos s_1}{2(k+s_1)} \right] + e^{-20s_2} J_0(s_2) \left[J_1(s_2) - \frac{k s_2 \cos s_2}{2(k+s_2)} \right] \right\}$$

$$- \frac{\pi}{F^2(s_3-s_4)} \left\{ e^{-20s_3} J_0(s_3) \left[J_1(s_3) - \frac{k s_3 \cos s_3}{2(k+s_3)} \right] - e^{-20s_4} J_0(s_4) \left[J_1(s_4) - \frac{k s_4 \cos s_4}{2(k+s_4)} \right] \right\}$$

$$\operatorname{Im}\{\tilde{C}_{01}\} = \int_0^\infty e^{-20s} J_0(s) \left\{ \frac{1}{F^2} \left[\frac{1}{(s-s_1)(s-s_2)} - \frac{1}{(s-s_3)(s-s_4)} \right] \right.$$

$$\left. + \frac{1}{2} s k \cos s \left[\frac{1}{k^2-s^2} + \frac{1}{F^2} \left(\frac{1}{(k-s)(s-s_3)(s-s_4)} - \frac{1}{(k+s)(s-s_1)(s-s_2)} \right) \right] \right\} ds$$

$$- \frac{k}{2} \int_1^\infty \frac{\cos[k(\xi-1)]}{\sqrt{\xi^2-1}} d\xi$$

$$- \frac{k\pi}{2F^2(s_1-s_2)} \left\{ \frac{s_1 e^{-20s_1} J_0(s_1) \sin s_1}{k+s_1} + \frac{s_2 e^{-20s_2} J_0(s_2) \sin s_2}{k+s_2} \right\}$$

$$+ \frac{k\pi}{2F^2(s_3-s_4)} \left\{ \frac{s_3 e^{-20s_3} J_0(s_3) \sin s_3}{k-s_3} - \frac{s_4 e^{-20s_4} J_0(s_4) \sin s_4}{k-s_4} \right\}$$

$$Re\{\tilde{C}_{0n}\} = \frac{n}{2}(-1)^{\frac{n}{2}}[1+(-1)^n] \int_0^\infty e^{-2Ds} J_0(s) J_n(s) \left\{ \frac{1}{s} + \frac{1}{F^2} \left[\frac{1}{(s-s_1)(s-s_2)} + \frac{1}{(s-s_3)(s-s_4)} \right] \right\} ds$$

$$+ \frac{n\pi}{2F^2}(-1)^{\frac{n+1}{2}}[1-(-1)^n] \left\{ \frac{1}{(s_1-s_2)} \left[e^{-2Ds_1} J_0(s_1) J_n(s_1) + e^{-2Ds_2} J_0(s_2) J_n(s_2) \right] \right.$$

$$\left. + \frac{1}{(s_3-s_4)} \left[e^{-2Ds_3} J_0(s_3) J_n(s_3) - e^{-2Ds_4} J_0(s_4) J_n(s_4) \right] \right\}$$

for $n = 2, 3, 4, \dots$

$$Im\{\tilde{C}_{0n}\} = \frac{-n}{2F^2}(-1)^{\frac{n+1}{2}}[1-(-1)^n] \int_0^\infty e^{-2Ds} J_0(s) J_n(s) \left[\frac{1}{(s-s_1)(s-s_2)} - \frac{1}{(s-s_3)(s-s_4)} \right] ds$$

$$+ \frac{n\pi}{2F^2}(-1)^{\frac{n+1}{2}}[1+(-1)^n] \left\{ \frac{1}{(s_1-s_2)} \left[e^{-2Ds_1} J_0(s_1) J_n(s_1) + e^{-2Ds_2} J_0(s_2) J_n(s_2) \right] \right.$$

$$\left. - \frac{1}{(s_3-s_4)} \left[e^{-2Ds_3} J_0(s_3) J_n(s_3) - e^{-2Ds_4} J_0(s_4) J_n(s_4) \right] \right\}$$

for $n = 2, 3, 4, \dots$

$$Re \{ \tilde{C}_{m0} \} = -(-1)^{\frac{m-1}{2}} [1 - (-1)^m] \int_0^\infty e^{-20s} J_m(s) \left\{ \left[1 + \frac{s}{F^2} \left(\frac{1}{(s-s_1)(s-s_2)} + \frac{1}{(s-s_3)(s-s_4)} \right) \right] J_0(s) \right.$$

$$\left. - k \cos s \left[\frac{k}{k^2 - s^2} + \frac{s}{F^2} \left(\frac{1}{(k+s)(s-s_1)(s-s_2)} + \frac{1}{(k-s)(s-s_3)(s-s_4)} \right) \right] \right\} ds$$

$$+ (-1)^{\frac{m}{2}} [1 + (-1)^m] \int_0^\infty e^{-20s} J_m(s) \left\{ \left[1 + \frac{s}{F^2} \left(\frac{1}{(s-s_1)(s-s_2)} + \frac{1}{(s-s_3)(s-s_4)} \right) \right] J_1(s) + k \sin s \left[\frac{k}{k^2 - s^2} \right. \right.$$

$$\left. \left. + \frac{s}{F^2} \left(\frac{1}{(k+s)(s-s_1)(s-s_2)} + \frac{1}{(k-s)(s-s_3)(s-s_4)} \right) \right] \right\} ds + 2k(-1)^m \int_1^\infty \frac{\sin [k(\xi-1)] (\xi - \sqrt{\xi^2-1})^m}{\sqrt{\xi^2-1}} d\xi$$

$$+ \frac{\pi}{F^2} (-1)^{\frac{m}{2}} [1 + (-1)^m] \left\{ \frac{1}{(s_1 - s_2)} \left[s_1 e^{-20s_1} J_m(s_1) \left(J_0(s_1) - \frac{k \cos s_1}{k+s_1} \right) + s_2 e^{-20s_2} J_m(s_2) \left(J_0(s_2) - \frac{k \cos s_2}{k+s_2} \right) \right] \right.$$

$$\left. + \frac{1}{(s_3 - s_4)} \left[s_3 e^{-20s_3} J_m(s_3) \left(J_0(s_3) - \frac{k \cos s_3}{k-s_3} \right) - s_4 e^{-20s_4} J_m(s_4) \left(J_0(s_4) - \frac{k \cos s_4}{k-s_4} \right) \right] \right\}$$

$$- \frac{\pi}{F^2} (-1)^{\frac{m+1}{2}} [1 - (-1)^m] \left\{ \frac{1}{(s_1 - s_2)} \left[s_1 e^{-20s_1} J_m(s_1) \left(J_1(s_1) + \frac{k \sin s_1}{k+s_1} \right) + s_2 e^{-20s_2} J_m(s_2) \left(J_1(s_2) + \frac{k \sin s_2}{k+s_2} \right) \right] \right.$$

$$\left. + \frac{1}{(s_3 - s_4)} \left[s_3 e^{-20s_3} J_m(s_3) \left(J_1(s_3) + \frac{k \sin s_3}{k-s_3} \right) - s_4 e^{-20s_4} J_m(s_4) \left(J_1(s_4) + \frac{k \sin s_4}{k-s_4} \right) \right] \right\}$$

for $m = 1, 2, 3, \dots$

$$J_m \left\{ \tilde{\zeta}_{m0} \right\} = (-1)^{\frac{m+1}{2}} [1+(-1)^m] \int_0^\infty s e^{-2Ds} J_m(s) \left\{ \frac{1}{F^2} \left[\frac{1}{(s-s_3)(s-s_4)} - \frac{1}{(s-s_1)(s-s_2)} \right] J_0(s) \right.$$

$$- K \cos s \left[\frac{1}{k^2 - s^2} + \frac{1}{F^2} \left(\frac{1}{(k-s)(s-s_3)(s-s_4)} - \frac{1}{(k+s)(s-s_1)(s-s_2)} \right) \right] \} ds$$

$$+ (-1)^{\frac{m-1}{2}} [1-(-1)^m] \int_0^\infty s e^{-2Ds} J_m(s) \left\{ \frac{1}{F^2} \left[\frac{1}{(s-s_3)(s-s_4)} - \frac{1}{(s-s_1)(s-s_2)} \right] J_1(s) + K \sin s \left[\frac{1}{k^2 - s^2} \right. \right.$$

$$+ \left. \frac{1}{F^2} \left(\frac{1}{(k-s)(s-s_3)(s-s_4)} - \frac{1}{(k+s)(s-s_1)(s-s_2)} \right) \right] \} ds + 2K(-1)^m \int_1^\infty \frac{\cos [k(\xi-1)] (\xi - \sqrt{\xi^2 - 1})^m}{\sqrt{\xi-1}} d\xi$$

$$+ \frac{\pi}{F^2} (-1)^{\frac{m+1}{2}} [1-(-1)^m] \left\{ \frac{1}{(s_1 - s_2)} \left[s_1 e^{-2Ds_1} J_m(s_1) \left(J_0(s_1) - \frac{K \cos s_1}{k+s_1} \right) + s_2 e^{-2Ds_2} J_m(s_2) \left(J_0(s_2) - \frac{K \cos s_2}{k+s_2} \right) \right. \right.$$

$$- \left. \frac{1}{(s_3 - s_4)} \left[s_3 e^{-2Ds_3} J_m(s_3) \left(J_0(s_3) - \frac{K \cos s_3}{k-s_3} \right) - s_4 e^{-2Ds_4} J_m(s_4) \left(J_0(s_4) - \frac{K \cos s_4}{k-s_4} \right) \right] \right\}$$

$$+ \frac{\pi}{F^2} (-1)^{\frac{m}{2}} [1+(-1)^m] \left\{ \frac{1}{(s_1 - s_2)} \left[s_1 e^{-2Ds_1} J_m(s_1) \left(J_1(s_1) + \frac{K \sin s_1}{k+s_1} \right) + s_2 e^{-2Ds_2} J_m(s_2) \left(J_1(s_2) + \frac{K \sin s_2}{k+s_2} \right) \right. \right]$$

$$- \left. \frac{1}{(s_3 - s_4)} \left[s_3 e^{-2Ds_3} J_m(s_3) \left(J_1(s_3) + \frac{K \sin s_3}{k-s_3} \right) - s_4 e^{-2Ds_4} J_m(s_4) \left(J_1(s_4) + \frac{K \sin s_4}{k-s_4} \right) \right] \right\}$$

for $m = 1, 2, 3, \dots$

$$\operatorname{Re}\{\tilde{C}_m\} = (-1)^{\frac{m+1}{2}} [1 - (-1)^m] \int_0^\infty e^{-2Ds} J_m(s) \left\{ \left[\frac{1}{s} + \frac{1}{F^2} \left(\frac{1}{(s-s_1)(s-s_2)} + \frac{1}{(s-s_3)(s-s_4)} \right) \right] J_1(s) \right.$$

$$\left. - \frac{1}{2} K \cos S \left[\frac{K}{K^2 - S^2} + \frac{S}{F^2} \left(\frac{1}{(K+S)(S-s_1)(S-s_2)} + \frac{1}{(K-S)(S-s_3)(S-s_4)} \right) \right] \right\} ds$$

$$+ \frac{K}{2} (-1)^{\frac{m}{2}} [1 + (-1)^m] \int_0^\infty e^{-2Ds} J_m(s) \sin S \left\{ \frac{K}{K^2 - S^2} + \frac{S}{F^2} \left[\frac{1}{(K+S)(S-s_1)(S-s_2)} + \frac{1}{(K-S)(S-s_3)(S-s_4)} \right] \right\} ds$$

$$+ K (-1)^m \int_1^\infty \frac{\sin [K(\xi-1)] (\xi - \sqrt{\xi^2 - 1})^m}{\sqrt{\xi^2 - 1}} d\xi$$

$$+ \frac{\pi}{F^2} (-1)^{\frac{m}{2}} [1 + (-1)^m] \left\{ \frac{1}{(s_1 - s_2)} \left[e^{-2Ds_1} J_m(s_1) \left(J_1(s_1) - \frac{KS_1 \cos S_1}{2(K+S_1)} \right) + e^{-2Ds_2} J_m(s_2) \left(J_1(s_2) - \frac{KS_2 \cos S_2}{2(K+S_2)} \right) \right] \right.$$

$$\left. + \frac{1}{(s_3 - s_4)} \left[e^{-2Ds_3} J_m(s_3) \left(J_1(s_3) - \frac{KS_3 \cos S_3}{2(K-S_3)} \right) - e^{-2Ds_4} J_m(s_4) \left(J_1(s_4) - \frac{KS_4 \cos S_4}{2(K-S_4)} \right) \right] \right\}$$

$$- \frac{\pi K}{2F^2} (-1)^{\frac{m+1}{2}} [1 - (-1)^m] \left\{ \frac{1}{(s_1 - s_2)} \left[\frac{s_1 e^{-2Ds_1} J_m(s_1) \sin S_1}{K + S_1} + \frac{s_2 e^{-2Ds_2} J_m(s_2) \sin S_2}{K + S_2} \right] \right.$$

$$\left. + \frac{1}{(s_3 - s_4)} \left[\frac{s_3 e^{-2Ds_3} J_m(s_3) \sin S_3}{K - S_3} - \frac{s_4 e^{-2Ds_4} J_m(s_4) \sin S_4}{K - S_4} \right] \right\}$$

for $m = 1, 2, 3, \dots$

$$\begin{aligned}
\Im\{C_m\} = & -(-1)^{\frac{m}{2}} [1+(-1)^m] \int_0^\infty e^{-2\alpha s} J_m(s) \left\{ \frac{1}{F^2} \left[\frac{1}{(s-s_1)(s-s_2)} - \frac{1}{(s-s_3)(s-s_4)} \right] J_1(s) \right. \\
& \left. + \frac{1}{2} s k \cos s \left[\frac{1}{k^2-s^2} + \frac{1}{F^2} \left(\frac{1}{(k-s)(s-s_3)(s-s_4)} - \frac{1}{(k+s)(s-s_1)(s-s_2)} \right) \right] \right\} ds \\
& - \frac{k}{2} (-1)^{\frac{m+1}{2}} [1-(-1)^m] \int_0^\infty s e^{-2\alpha s} J_m(s) \sin s \left\{ \frac{1}{k^2-s^2} \right. \\
& \left. + \frac{1}{F^2} \left[\frac{1}{(k-s)(s-s_3)(s-s_4)} - \frac{1}{(k+s)(s-s_1)(s-s_2)} \right] \right\} ds + k(-1)^m \int_1^\infty \frac{\cos [k(\xi-1)] (\xi - \sqrt{\xi^2-1})^m}{\sqrt{\xi^2-1}} d\xi \\
& + \frac{\pi}{F^2} (-1)^{\frac{m+1}{2}} [1-(-1)^m] \left\{ \frac{1}{(s_1-s_2)} \left[e^{-2\alpha s_1} J_m(s_1) \left(J_1(s_1) - \frac{KS_1 \cos S_1}{2(k+S_1)} \right) + e^{-2\alpha s_2} J_m(s_2) \left(J_1(s_2) - \frac{KS_2 \cos S_2}{2(k+S_2)} \right) \right] \right. \\
& \left. - \frac{1}{(s_3-s_4)} \left[e^{-2\alpha s_3} J_m(s_3) \left(J_1(s_3) - \frac{KS_3 \cos S_3}{2(k-S_3)} \right) - e^{-2\alpha s_4} J_m(s_4) \left(J_1(s_4) - \frac{KS_4 \cos S_4}{2(k-S_4)} \right) \right] \right\} \\
& + \frac{\pi k}{2F^2} (-1)^{\frac{m}{2}} [1+(-1)^m] \left\{ \frac{1}{(s_1-s_2)} \left[\frac{s_1 e^{-2\alpha s_1} J_m(s_1) \sin S_1}{k+S_1} + \frac{s_2 e^{-2\alpha s_2} J_m(s_2) \sin S_2}{k+S_2} \right] \right. \\
& \left. - \frac{1}{(s_3-s_4)} \left[\frac{s_3 e^{-2\alpha s_3} J_m(s_3) \sin S_3}{k-S_3} - \frac{s_4 e^{-2\alpha s_4} J_m(s_4) \sin S_4}{k-S_4} \right] \right\}
\end{aligned}$$

for $m = 1, 2, 3, \dots$

$$\operatorname{Re}\{\tilde{C}_{mn}\} = -(-1)^{\frac{m+n}{2}} [(-1)^m + (-1)^n] n \int_0^\infty e^{-20s} J_m(s) \bar{J}_n(s) \left\{ \frac{1}{s} + \frac{1}{F^2} \left[\frac{1}{(s-s_1)(s-s_2)} + \frac{1}{(s-s_3)(s-s_4)} \right] \right\} ds$$

$$\begin{aligned} & - \frac{n\pi}{F^2} (-1)^{\frac{m+n+1}{2}} [(-1)^m - (-1)^n] \left\{ \frac{1}{(s_1-s_2)} \left[e^{-20s_1} \bar{J}_m(s_1) \bar{J}_n(s_1) + e^{-20s_2} \bar{J}_m(s_2) \bar{J}_n(s_2) \right] \right. \\ & \left. + \frac{1}{(s_3-s_4)} \left[e^{-20s_3} \bar{J}_m(s_3) \bar{J}_n(s_3) - e^{-20s_4} \bar{J}_m(s_4) \bar{J}_n(s_4) \right] \right\} \end{aligned}$$

for $m = 1, 2, 3, \dots$ and $n = 2, 3, 4, \dots$

$$\operatorname{Im}\{\tilde{C}_{mn}\} = \frac{n}{F^2} (-1)^{\frac{m+n+1}{2}} [(-1)^m - (-1)^n] \int_0^\infty e^{-20s} J_m(s) \bar{J}_n(s) \left[\frac{1}{(s-s_1)(s-s_2)} - \frac{1}{(s-s_3)(s-s_4)} \right] ds$$

$$\begin{aligned} & - \frac{n\pi}{F^2} (-1)^{\frac{m+n}{2}} [(-1)^m + (-1)^n] \left\{ \frac{1}{(s_1-s_2)} \left[e^{-20s_1} J_m(s_1) J_n(s_1) + e^{-20s_2} J_m(s_2) J_n(s_2) \right] \right. \\ & \left. - \frac{1}{(s_3-s_4)} \left[e^{-20s_3} J_m(s_3) J_n(s_3) - e^{-20s_4} J_m(s_4) J_n(s_4) \right] \right\} \end{aligned}$$

for $m = 1, 2, 3, \dots$ and $n = 2, 3, 4, \dots$

APPENDIX C

$\Delta p(\theta, t)$ FOR THE CASE IN WHICH $D \rightarrow \infty$

It has already been mentioned that for $D \rightarrow \infty$, equation (1.46) reduces to

$$\frac{1}{2\pi} \int_{-1}^1 \frac{g(\xi)}{x - \xi} d\xi = \frac{i\kappa \bar{\Gamma}}{2\pi} \int_1^\infty \frac{e^{-i\kappa(\xi-1)}}{\xi - x} d\xi + G^*(x), \quad (C1)$$

where

$$G^*(x) = U [H'(x) + i\kappa H(x)], \quad (C2)$$

and depends upon the motion imposed on the plate.

If D is allowed to approach infinity in the equations for the \tilde{C}_{mn} of Appendix B, the only remaining terms are

$$\tilde{C}_{\infty\infty} = -i\kappa \int_1^\infty \frac{e^{-i\kappa(\xi-1)}}{\sqrt{\xi^2 - 1}} d\xi, \quad (C3)$$

$$\tilde{C}_{\infty 1} = -\frac{i\kappa}{2} \int_1^\infty \frac{e^{-i\kappa(\xi-1)}}{\sqrt{\xi^2 - 1}} d\xi, \quad (C4)$$

$$\tilde{C}_{m\infty} = 2i\kappa(-1)^m \int_1^\infty \frac{(\xi - \sqrt{\xi^2 - 1})^m e^{-i\kappa(\xi-1)}}{\sqrt{\xi^2 - 1}} d\xi, \quad (C5)$$

$$\tilde{C}_{m1} = i \kappa (-1)^m \int_1^\infty \frac{(\xi - \sqrt{\xi^2 - 1})^m e^{-i \kappa (\xi - 1)}}{\sqrt{\xi^2 - 1}} d\xi. \quad (C6)$$

It is easy to see that

$$\begin{aligned} \tilde{C}_{00} &= 2 \tilde{C}_{01}, \\ \tilde{C}_{10} &= 2 \tilde{C}_{11}, \\ &\vdots \\ \tilde{C}_{m0} &= 2 \tilde{C}_{m1}, \end{aligned}, \quad (C7)$$

and that the infinite system of equations

$$a_m = \sum_{n=0}^{\infty} \tilde{C}_{mn} a_n + r_m, \quad m = 0, 1, 2, \dots \quad (C8)$$

may be decoupled and solved to yield

$$a_0 = r_0 \left(\frac{1 - \tilde{C}_{11}}{1 - 2 \tilde{C}_{01} - \tilde{C}_{11}} \right) + r_1 \left(\frac{\tilde{C}_{01}}{1 - 2 \tilde{C}_{01} - \tilde{C}_{11}} \right), \quad (C9)$$

$$a_1 = r_0 \left(\frac{2 \tilde{C}_{11}}{1 - 2 \tilde{C}_{01} - \tilde{C}_{11}} \right) + r_1 \left(\frac{1 - 2 \tilde{C}_{01}}{1 - 2 \tilde{C}_{01} - \tilde{C}_{11}} \right). \quad (C10)$$

Then

$$a_n = \tilde{C}_{n0} a_0 + \tilde{C}_{n1} a_1 + r_n, \quad n \geq 2. \quad (C11)$$

It is desired to write these a_n in terms of the Fourier coefficients, A_n , of that portion of the downwash which was expanded. Thus, it is expected that the pressure difference

$$\Delta p(\theta, t) = 2\rho U^2 e^{i\omega t} \left\{ a_0 \cot \frac{\theta}{2} + \left(a_1 + ik [3a_0 + a_1 + \frac{a_2}{2}] \right) \sin \theta + \right. \\ \left. + \sum_n \left[\left\{ a_n + \frac{ik}{2n} (a_{n+1} - a_{n-1} + z(z a_0 + a_1)(-1)^{n+1}) \right\} \sin n\theta \right] \right\} \quad (C12)$$

will also be expressible in terms of the coefficients A_n .

First we calculate the values of \tilde{C}_{11} and \tilde{C}_{01} by a change of the variable. Let

$$\xi = \cosh \theta,$$

so that

$$\tilde{C}_{01} = -\frac{ik}{2} e^{ik} \int_0^\infty e^{-ik \cosh \theta} \sin n\theta \, d\theta \\ = -\frac{ik}{2} e^{ik} K_0(ik), \quad (C13)$$

where $K_0(ik)$ is the modified Bessel function of the second kind. To justify this notation, we look first at the integral

$$K_n(z) = \int_0^\infty e^{-z \cosh \theta} \cosh n\theta \, d\theta, \quad \operatorname{Re}(z) > 0,$$

where $z = x + iy$. This integral diverges for pure imaginary z . Thus, we need to find the limit of the integral as $x \rightarrow 0$. Proceeding with this, we note from Watson [26] that

$$K_n(z) = \frac{\pi}{2} i^{-n-1} H_n^{(2)}(-iz),$$

where $H_n^{(2)}(-iz)$ is a Hankel function defined by

$$H_n^{(2)}(-iz) = J_n(-iz) - i Y_n(-iz).$$

$J_n(-iz)$ and $Y_n(-iz)$ are n^{th} order Bessel and Neumann functions respectively. Then, for $x > 0$

$$K_n(x+iy) = \frac{\pi}{2} i^{-n-1} \left[J_n(y-ix) - i Y_n(y-ix) \right].$$

Hence, taking the limit as follows,

$$\begin{aligned} \lim_{x \rightarrow 0^+} K_n(x+iy) &= \lim_{x \rightarrow 0^+} \int_0^\infty e^{-(x+iy)\cosh \theta} \cosh n\theta d\theta \\ &= \frac{\pi}{2} i^{-n-1} [J_n(y) - i Y_n(y)] \\ &= \frac{\pi}{2} i^{-n-1} H_n^{(2)}(y) \end{aligned}$$

Now, as it has been shown that

$$\lim_{x \rightarrow 0^+} K_n(x+iy)$$

is a well-behaved function, the notation $K_n(iy)$ will be used in a manipulative sense in what follows.

A calculation similar to that leading to (C13) yields

$$\tilde{C}_1 = -ik e^{ik} K(iK) + 1. \quad (\text{C14})$$

Substituting (C13) and (C14) into (C9), we obtain

$$a_0 = \frac{A_0}{2} C(k) + \frac{A_1}{2} [1 - C(k)], \quad (\text{C15})$$

where $C(k)$ is Theodorsen's function [30]. $C(k)$ may be given by

$$C(k) = \frac{H_1^{(2)}(k)}{H_1^{(2)}(k) + i H_0^{(2)}(k)} = \frac{K_1(iK)}{K_1(iK) + K_0(iK)}. \quad (\text{C16})$$

Note also that we have made use of equations (2.16), relating the values of the \tilde{C}_m to the A_m .

Next the coefficient of $\sin \theta$ in (C12) is investigated. Noting that

$$\tilde{C}_{21} = ik e^{ik} K_0^{(ik)} + 2e^{ik} K_1^{(ik)} + \frac{2i}{k} - 2, \quad (C17)$$

the coefficient

$$[\alpha_1 + ik(3\alpha_0 + \alpha_1 + \frac{\alpha_2}{z})], \quad (C18)$$

may be written as

$$-A_n + \frac{ik}{2n} [A_{n-1} - A_{n+1}]. \quad (C19)$$

Finally, we establish that the coefficient of $\sin n\theta$ may be written as

$$-A_n + \frac{ik}{2n} [A_{n-1} - A_{n+1}]. \quad (C20)$$

As this is somewhat more difficult, some details will be given. From (C11) and (2.16) we write

$$\alpha_n = \tilde{C}_{n1} (2\alpha_0 + \alpha_1) - A_n. \quad (C21)$$

Then

$$\alpha_{n+1} = \tilde{C}_{n+1,1} (2\alpha_0 + \alpha_1) - A_{n+1}, \quad (C22)$$

$$\alpha_{n-1} = \tilde{C}_{n-1,1} (2\alpha_0 + \alpha_1) - A_{n-1}. \quad (C23)$$

Substituting these values for α_n , α_{n+1} , and α_{n-1} into the expression for the coefficient of $\sin n\theta$ from (C12), we obtain

$$\begin{aligned}\tilde{C}_{n_1}(za_0 + a_1) - A_n + \frac{ik}{zn} \left[\tilde{C}_{n+1,1}(za_0 + a_1) - A_{n+1} + \right. \\ \left. A_{n-1} - \tilde{C}_{n-1,1}(za_0 + a_1) + z(za_0 + a_1)(-1)^{n+1} \right],\end{aligned}$$

which may be written as

$$\begin{aligned}-A_n + \frac{ik}{zn} [A_{n-1} - A_{n+1}] + \tilde{C}_{n_1}(za_0 + a_1) + \\ + \frac{ik}{zn} [(\tilde{C}_{n+1,1} - \tilde{C}_{n-1,1})(za_0 + a_1) + z(za_0 + a_1)(-1)^{n+1}].\end{aligned}$$

Thus, we try to show that

$$\tilde{C}_{n_1} + \frac{ik}{zn} [(\tilde{C}_{n+1,1} - \tilde{C}_{n-1,1}) + z(-1)^{n+1}] (za_0 + a_1) = 0 \quad (C24)$$

in accordance with (C20). This is equivalent to showing that

$$\tilde{C}_{n_1} + \frac{ik}{zn} [\tilde{C}_{n+1,1} - \tilde{C}_{n-1,1} + z(-1)^{n+1}] = 0 \quad (C25)$$

as $(2a_0 + a_1)$ is presumably not zero. Using the integral values for \tilde{C}_{n_1} , $\tilde{C}_{n+1,1}$, and $\tilde{C}_{n-1,1}$ as given by (C6), equation (C25) may be written, after some manipulation, as

$$\int_1^\infty \frac{(\xi - \sqrt{\xi^2 - 1})^n}{\sqrt{\xi^2 - 1}} [n + ik\sqrt{\xi^2 - 1}] e^{-ik\xi} d\xi = e^{-ik}. \quad (C26)$$

Again letting $\xi = \cosh \theta$, we write for (C26)

$$\int_0^\infty (\cosh n\theta - \sinh n\theta)(n + ik \sinh \theta) e^{-ik \cosh \theta} d\theta = e^{-ik},$$

or

$$\begin{aligned}
 & n \int_0^\infty e^{-ik \cosh \theta} \cosh n\theta d\theta - n \int_0^\infty e^{-ik \cosh \theta} \sinh n\theta d\theta + \\
 & + ik \int_0^\infty e^{-ik \cosh \theta} \cosh n\theta \sinh \theta d\theta - ik \int_0^\infty e^{-ik \cosh \theta} \sinh n\theta \sinh \theta d\theta = e^{-ik}. \quad (C27)
 \end{aligned}$$

Integrating the second integral in (C27) by parts, we obtain for the entire equation

$$n K_n(ik) - \frac{\cosh n\theta}{e^{ik \cosh \theta}} \Big|_0^\infty - ik \int_0^\infty e^{-ik \cosh \theta} \sinh n\theta \sinh \theta d\theta = e^{-ik}. \quad (C28)$$

Now using the identity

$$\sinh n\theta \sinh \theta = \frac{1}{2} [\cosh(n+1)\theta - \cosh(n-1)\theta]$$

in (C28), we have after integration

$$n K_n(ik) + e^{-ik} - \frac{ik}{2} [K_{n+1}(ik) - K_{n-1}(ik)] = e^{-ik}. \quad (C29)$$

The recursion identity

$$K_n(ik) = \frac{ik}{2n} [K_{n+1}(ik) - K_{n-1}(ik)]$$

allows us to conclude that

$$e^{-ik} = e^{-ik},$$

and that (C24) is valid. Hence, the pressure difference distribution may be written as follows for the case $D \rightarrow \infty$:

$$\Delta p(\theta, t) = 2\rho U^2 e^{i\omega t} \left\{ \overset{*}{a}_0 \cot \frac{\theta}{2} + \sum_{n=1}^{\infty} \overset{*}{a}_n \sin n\theta \right\} , \quad (C30)$$

where

$$\overset{*}{a}_0 = \frac{A_0}{2} C(k) + \frac{A_1}{2} [1 - C(k)] , \quad (C31)$$

$$\overset{*}{a}_n = -A_n + \frac{i k}{2n} [A_{n-1} - A_{n+1}] . \quad (C32)$$

This expression for $\Delta p(\theta, t)$ is equivalent to that obtained by Siekmann [8]. Note that the Fourier coefficients, A_n , of this paper and those used by Siekmann, $\overset{*}{A}_n$, are related by

$$A_n = 2 \overset{*}{A}_n$$

and that Siekmann calls the pressure difference $\Delta \Pi(\theta, t)$.

It is also possible to reduce equation (3.55) for the thrust to that obtained by Siekmann, using techniques similar to those above.

LIST OF REFERENCES

1. R. W. L. Gawn, "Aspects of the Locomotion of Whales," Nature (London), Vol. 161 (1948), p. 44.
2. R. W. L. Gawn, "Fish Propulsion in Relation to Ship Design," Trans. Inst. Nav. Arch. (1950), p. 323.
3. Sir Geoffrey I. Taylor, "The Action of Waving Cylindrical Tails in Propelling Microscopic Organisms," Proc. Roy. Soc. Lond., A 211 (1951), p. 158.
4. Sir Geoffrey I. Taylor, "Analysis of the Swimming of Long and Narrow Animals," Proc. Roy. Soc. Lond., A 214 (1952), p. 158.
5. Sir James Gray, "How Fishes Swim," Sci. Am. (August, 1957), p. 48.
6. E. G. Richardson, "The Physical Aspects of Fish Propulsion," Jour. Exp. Biol., Vol. 13, No. 1 (1936), p. 63.
7. H. E. Dickmann, "Wie schwimmen Fische," Umschau, Vol. 53, No. 10 (1953), p. 304.
8. J. Siekmann, "Theoretical Studies of Sea Animal Locomotion, Part 1," Ing. -Arch., Bd. 31 (1962), p. 214; "Theoretical Studies of Sea Animal Locomotion, Part 2," Ing. -Arch., Bd. 32 (1963), p. 40.
9. T. Y. Wu, "Swimming of a Waving Plate," Jour. Fluid Mech., Vol. 10 (1961), p. 321.
10. H. G. Küssner and L. Schwarz, "The Oscillating Wing With Aerodynamically Balanced Elevator," Luftfahrtforschung, 17 (1940), p. 377. (English translation: NACA TM 991, 1941.)
11. L. Schwarz, "Berechnung der Druckverteilung einer harmonisch sich verformenden Tragfläche in ebener Stromung," Luftfahrtforschung, 17 (1940), p. 379.

12. E. H. Smith and D. E. Stone, "Perfect Fluid Forces in Fish Propulsion: The Solution of the Problem in an Elliptic Cylinder Co-ordinate System," Proc. Roy. Soc. Lond., A 261 (1961), p. 316.
13. S. K. Pao and J. Siekmann, "Note on the Smith-Stone Theory of Fish Propulsion," submitted to the Proc. Roy. Soc. Lond.
14. P. Crimi and I. C. Statler, "Forces and Moments on an Oscillating Hydrofoil," Cornell Aeronautical Laboratory Report No. BB-1629-S-1 (1962).
15. H. S. Tan, "On Source and Vortex of Fluctuating Strength Travelling Beneath a Free Surface," Quart. Appl. Math., Vol. 13, No. 3 (1955), p. 314.
16. H. S. Tan, "Waves Produced by a Pulsating Source Travelling Beneath a Free Surface," Quart. Appl. Math., Vol. 15, No. 3 (1957), p. 249.
17. A. Robinson and J. A. Laurmann, Wing Theory, Cambridge University Press, England (1956).
18. H. Söhngen, "Die Lösungen der Integralgleichung $y(x) = \frac{1}{2\pi} \int_{-a}^a \frac{f(\xi)}{x-\xi} d\xi$ und deren Anwendungen in der Tragflügeltheorie," Math. Z., Vol. 45 (1939), p. 245.
19. W. H. Chu and H. N. Abramson, "Effect of the Free Surface on the Flutter of Submerged Hydrofoils," Jour. Ship Res., Vol. 3, No. 1 (1959).
20. P. Kaplan, "A Hydrodynamic Theory for the Forces on Hydrofoils in Unsteady Motion," Doctoral Dissertation, Stevens Institute of Technology (1955).
21. L. M. Milne-Thomson, Theoretical Hydrodynamics, 2d ed., The Macmillan Company, New York (1960).
22. Lord Rayleigh, "The Form of Standing Waves on the Surface of Running Water," Proc. Lond. Math. Soc., Vol. 15 (1883), p. 69.
23. W. H. Isay, "Zur Theorie der nahe der Wasseroberflächen fahrenden Tragflächen," Ing. -Arch., Bd. 27 (1960), p. 295.

24. L. V. Kantorovich and V. I. Krylov, Approximate Methods of Higher Analysis, Interscience Publishers, Inc., New York (1958).
25. H. Wagner, "Über die Entstehung der dynamischen Auftriebes von Tragflügeln," A. Angew. Math. Mech., 5 (1925), p. 17.
26. G. N. Watson, A Treatise on the Theory of Bessel Functions, 2d ed., Cambridge University Press, England (1944).
27. W. E. Milne, Numerical Calculus, Princeton University Press, New Jersey (1949).
28. Sir Horace Lamb, Hydrodynamics, 6th ed., Dover Publications, New York (1932).
29. I. N. Sneddon, Elements of Partial Differential Equations, McGraw-Hill Book Company, Inc., New York (1957).
30. Y. Luke and M. A. Dengler, "Tables of the Theodorsen Circulation Function for Generalized Motion," Jour. Aero. Sci., Vol. 18 (1951), p. 478.

BIOGRAPHICAL SKETCH

Joe Wilson Reece was born on March 1, 1935, in Elkin, North Carolina. He was graduated from Boonville High School, Boonville, North Carolina, in May, 1953. In June, 1957, he received the degree of Bachelor of Nuclear Engineering from North Carolina State College. He worked during the academic year 1957-1958 as a graduate assistant in the Department of Mathematics. From 1958 to 1961 he taught as an Instructor of Engineering Mechanics. In June, 1961, he received the degree of Master of Science in Applied Mathematics. In September, 1961, he entered the Graduate School of the University of Florida, where he has pursued his work as a Ford Foundation Fellow until the present time toward the degree of Doctor of Philosophy.

Joe Reece is married to the former Nancy Lee Fletcher and is the father of two children. He is a member of Theta Tau, Phi Kappa Phi, Tau Beta Pi, Sigma Pi Sigma, and Phi Eta Sigma.

This dissertation was prepared under the direction of the chairman of the candidate's supervisory committee and has been approved by all members of that committee. It was submitted to the Dean of the College of Engineering and to the Graduate Council, and was approved as partial fulfillment of the requirements for the degree of Doctor of Philosophy.

December, 1963

Thomas L. Martin Jr.
Dean, College of Engineering

Dean, Graduate School

Supervisory Committee:

I. Hermann

Chairman

W. A. Mark

S. S. Lu

Frederick K. Eliash

C. B. Smith

— 11th — 3